P–T Alpine metamorphic evolution of the Monte Rosa nappe along the Piedmont Zone boundary (Gressoney Valley, NW Italy)

Published version:

DOI:doi.org/10.1016/j.lithos.2011.09.007

(Article begins on next page)

P-T Alpine metamorphic evolution for the Monte Rosa Nappe along the Piedmont Zone boundary (Gressoney Valley, NW Alps)

Ivano Gasco[1*], Alessandro Borghi[2], Marco Gattiglio[1]

[1] Dipartimento di Scienze della Terra, Università degli Studi di Torino, Via Valperga Caluso 35, I-10125 Torino, Italy

[2] Dipartimento di Scienze Mineralogiche e Petrologiche, Università dedli Studi di Torino, Via Valperga Caluso 35, I-10125 Torino, Italy

*Corresponding author: ivano.gasco@yahoo.com

Abstract. The pseudosection modelling of two chemical systems (both metabasic and metapelitic) allowed to reconstruct the exhumation PT path followed by the southern slope of the Monte Rosa Nappe (Upper Gressoney Valley) during the Alpine orogenesis. The metamorphic evolution of the polymetamorphic basement complex from the Monte Rosa Nappe is marked by texturally distinct mineral assemblages, defining four Alpine metamorphic stages (M1, M2, M3 and M4) developed under different PT conditions. In particular, well preserved eclogitic boudins (M1 and M2 assemblages) were investigated to reconstruct the HP history related to the subduction event, while re-equilibrated metapelites allowed to infer the PT conditions attained during the development of the regional foliation (M3 and M4 assemblages). The HP event (M1) occurred at 550-570 °C and 24-27 kbar and is characterized by the assemblage Omp + Grt + Lws + Phe + Qtz + Gln ± Tlc in the eclogites. The M2 metamorphic stage consists of the assemblage Omp + Grt + Barr + Zo + Phe + Pg + Qtz and developed at 590-630 °C and 14.5-16.5 kbar suggesting a T increasing during decompression. After a further decompressional stage associated with a T decrease, the M3 tectono-metamorphic event developed syn-kinematically with the main regional foliation S_1. It is marked by the assemblage Phe + Pg + Grt + Chl + Ab/Olig + Hbl + Qtz + Rt/Ilm ± Bt in metapelites and by Cam (blue-green) + Chl + Ab + Bt + Qtz + Rt in the re-equilibrated metabasite boudins. It developed during increasing T (from 550 to ca. 600°C) and P (from 7 to 9 kbar). Finally, the M4 assemblage grew as rim over the M3 minerals or overgrew the S_1 regional foliation (albite porphyroblasts overgrowing the S_1 foliation already defined by albite) and therefore can be considered as the final stage of the M3 tectono-metamorphic event. From this data a different P-T path is proposed for the Monte Rosa Nappe compared to previous works. In particular, it shows a post-eclogitic decompression trajectory up to 7 kbar, followed by a P-T increase that can be related

to multiple burial–exhumation cycles during alpine orogenesis, as recently reported in literature for other Alpine units.

Keywords: Alpine metamorphism, pseudosection, PT path, Monte Rosa Nappe, Western Italian Alps.

1. Introduction

The axial portion of the Western Italian Alps (Austroalpine and Penninic Domains) represents a fossil subduction complex developed during the Alpine orogenic cycle. In the last twenty years, many geological transects (e.g. Pognante *et al.* 1987; Inger and Ramsbotham, 1997; Bucher *et al.*, 2004; Keller *et al.*, 2005) have improved our knowledge of the structural and metamorphic framework of the Western Alps. In the last years, numerous Authors, based on thermodynamic models, reported the P-T conditions reached during the metamorphic peak of the subduction event for the Gran Paradiso (Le Bayon *et al.*, 2006; Gabudianu *et al.*, 2009; Gasco *et al.*, 2010) and the Dora Maira (Chopin, 1984; Chopin *et al.*, 1991; Castelli *et al.*, 2007; Gasco *et al.*, in press) Massifs. Instead, for the Monte Rosa Nappe no recently reconstruction of P-T paths by means of the analysis of phase equilibria is performed, with exception of the Mg-riched metapelites system of whiteschist (Le Bayon *et al.*, 2000; 2006). For this reason, an apparent disagreement currently exist between P-T conditions reported for the Monte Rosa Nappe and the other Internal Crystalline Massifs (Gran Paradiso and Dora-Maira), despite their common Alpine tectono-metamorphic evolution.

This work aims to reconstruct the exhumation PT path of the Monte Rosa Nappe based on the pseudosection approach. The PEPLEX thermodynamic model of Connolly (1990) was applied to selected metabasic and metapelitic rocks in order to estimate the PT conditions attained during the eclogitic peak metamorphic event and to better constrain the PT path followed during the exhumation. Two different chemical systems have been investigated because of their tendency to register different stage of the metamorphic evolution. Generally, the basic system preserves very well the HP climax while the pelitic one records the last stages of the tectonometamorphic evolution. The studied rocks contain well preserved evidence of different high pressure stages that allowed to reconstruct the early-Alpine subduction event for the Monte Rosa Nappe. Phase diagrams modelling has also permitted to reconstruct the exhumation portion of the Alpine PT path on the base of the garnet growth zoning and on the chemical composition and micro-structural relationships with other minerals.

2. Geological setting

The Monte Rosa Nappe, together with the Dora Maira and the Gran Paradiso Massifs, represent continental basement Nappes of the inner Penninic Domain (e.g. Schmid *et al.*, 2004) in the Western Italian Alps, and are characterized by the occurrence of high pressure (HP) and in the case of Dora Maira Massif ultra-high pressure (UHP) metamorphic assemblages. They are known as the Internal Crystalline Massifs ([redacted]) and represent the deepest tectonic elements of the western Alps, which crop out as large axial culminations, thrusted by different structural elements of the Piedmont Zone.

The Monte Rosa Nappe (Bearth, 1952; Dal Piaz, 2001 for a review; [redacted] consists of pre-Alpine basement composed of a high-grade (biotite + sillimanite + k-feldspar assemblages and cordierite anatexites) paragneisses complex characterized by the occurence of anatectic melts, which was transformed into garnet-micaschists during the Alpine event (Dal Piaz, 2001). A composite Late Paleozoic batolith with granite to granodiorite composition intruded the paragneisses in the Late Carboniferous (310-330 Ma; Hunziker., 1970; Frey *et al.*, 1976; Engi *et al.*, 2001), while Permian ages (260-270 Ma; Lange *et al.*, 2000; Engi *et al.*, 2001) have been attributed to late magmatic stages. The whole nappe is characterized by low-strain domains which preserves intrusive relationships between the granitoids and the high-grade pre-alpine complex, and by high-strain domains in which the Alpine structural and metamorphic imprint is well developed (Dal Piaz, 1964, 1966, 1971;). Horizons rich of mafic boudins and marbles are present at different structural levels within the metapelites and are known as Furgg Zone s.s. (Bearth, 1952, 1954) in the northern part of the Nappe and southern Furgg Zone (Dal Piaz, 1964, 1966) on the Italian side. While the southern Furgg Zone is considered as a pre-Permian metamorphic complex (Dal Piaz, 2001), the interpretation of the Furgg Zone *s.s.* is very contrasting: Froitzheim (2001), Liati *et al.* (2001) and Kramer (2002) considered it as a Mesozoic tectonic mélange while Jaboyedoff *et al.* (1996) and Keller and Schmid (2001) suggested that it is an highly deformed stratigraphic sequence of Permo-Triassic cover and continental basement, intruded by post-Triassic mafic dykes. The post-Variscan cover of the Monte Rosa is represented by Late-Carboniferous-Permian and Mesozoic sequences mainly preserved in the external parts of the Nappe (Gornergrat Zone) or included in the Furgg Zone *s.s.* (Jaboyedoff *et al.*, 1996; Escher *et al.*, 1997). High pressure relics referred to the Alpine event consist of eclogite boudins and phengite-garnet-kyanite assemblages within the paragneisses, and of phengite-talc-chloritoid-chlorite-kyanite-quartz schists (whiteschist) along shear zones within the orthogneisses (Dal Piaz and Lombardo, 1986).

The eclogite facies metamorphic conditions have been estimated with classical thermobarometry giving ca 16 kbar & 500°C (Chopin and Monié, 1984), 10 ± 2 kbar and 500 ± 50 °C (Dal Piaz and Lombardo, 1986; Borghi *et al.*,1996) and 13-20 kbar and 535-620 °C (Ferrando, 2002; Ferrando *et al.*, 2002) in the southern part of the Nappe.

Lapen *et al.* (2007) reported similar results (P > 13 kbar and 480-570 °C obtained with classical thermobarometry) for quartz-phengite-carbonate-rutile veins crosscutting eclogite boudins, within the southern Furgg Zone. These veins were dated by U/Pb geochronology on rutile giving a minimum age of 42.6 ± 0.6 Ma for the eclogite facies event (Lapen *et al.*, 2007). In the central and the northeastern part of the Nappe, Engi *et al.* (2001) reported an age of 36 ± 6 (Th/U/Pb on monazite with most of the accurate ages at 32-38 Ma) for an high pressure stage during exhumation at 9-12 kbar for T data grouping at 580-620 °C and 730-755 °C, without any correlation with the regional gradient. A late-Alpine thermal overprinting is evidenced by monazite ages at 25-27 Ma (Engi *et al.*, 2001). The Alpine peak-pressure conditions estimated with the pseudosection approach for talc-chloritoid-phengite-quartz whiteschist gave 25 kbar and 580 °C (Le Bayon *et al.* 2000) and 24 ± 3 kbar and 505 ± 30 °C followed by decompression to 8 ± 3 kbar and 475 ± 30 °C (Le Bayon *et al.* 2006).

3. Tectonic setting

New detailed mapping at the 1:10000 scale was performed along the southern border of the Monte Rosa Nappe along the watershed between Gressoney and Ayas Valley and allowed to reconstruct its structural setting (Gasco and Gattiglio, 2011). A simplified map of the study area is reported in [redacted] where the deepest outcropping [redacted] is the Monte Rosa Nappe which is geometrically overlain, at the regional scale, by the Zermatt-Saas Unit.

The Monte Rosa Nappe mainly consists of a polymetamorphic complex including medium to coarse-grained garnet micaschists with the following main assemblage: Qtz + Wm + Chl + Ab + Grt (abbreviations of minerals are given according to Kretz,1983 ~~with the~~ [redacted] ~~of~~ by Bucher and Frey, 2002). The garnet micaschists show many intercalations of metabasite boudins which locally are arranged along layers parallel to the regional foliation (Fig. 3a) and minor layers of meta-intrusives comprising orthogneisses and aplitic dykes. Metabasites consist of well-preserved eclogites and re-equilibrated epidote-albite amphibolites. Other intercalations within the garnet micaschists are represented by albite micaschists poor of garnet and by fine-grained graphite-bearing micaschists. Both albite and graphite micaschists show transitional contact towards the garnet micaschists (Fig. 3b) and are considered to be stratigraphic intercalations within an heterogeneous pre-Alpine basement. Locally Bt + Grt rich dark nodules in a light quartz-feldspatic matrix were observed and were interpreted as stretched restitic portion of a partial melting process of pre-Alpine age (Fig. 3c).

The Zermatt-Saas Unit consists of a stack of tectonic slices comprising ultrabasic and basic rocks rarely overlain by a thin stratigraphic cover. The ultramafic rocks consist of foliated serpentinites that locally show thin layers (max 50-60 cm thick) of meta-rodingites (Fig. 3d) and boudins of eclogites, while the metabasites comprise medium to coarse-grained Mg-Al metagabbros, epidote-albite amphibolites and eclogites interpreted as Fe-Ti metagabbros or metabasalts. Eclogites consists of coherent bodies 100 m long and of boudins (20 cm to 5 m) within reequilibrated epidote-albite amphibolites. The Mesozoic cover sequence is scarce in the study area and mainly consists of ~~by~~ garnet calcschists interposed with impure marbles and by subordinate micaschists and greenstones (layered Ab + Chl + Act + Ep schists interpreted as submarine volcanics). The tectonic contact between Monte Rosa [redacted]d the Zermatt-Saas in marked by mylonitic micaschists with S-C structures with a foliation defined by Chl + Wm + Qtz + Grt + Hbl + Rt ± Ab and by rare serpentinite lenses and Chl-Act schists derived from the [redacted] metabasites or serpentinites. The mylonitic foliation in the [redacted] micaschists shows almost the same assemblage which define the S_1 foliation. The deformation zone is always in the range of 1-10 m thick and no eclogite facies assemblage has been observed along the contact.

4. Petrography and mineral chemistry

In order to constrain the metamorphic evolution of the southern border of the Monte Rosa Nappe, about thirty samples (micaschists and metabasites) were studied. [redacted] field study and petrographic investigation of selected samples, reveal that generally metapelites with a well developed regional foliation registered the reequilibration stage, while the eclogite facies assemblages are better preserved in the metabasite boudins. Two samples have been selected (Fig. 2) for pseudosection modelling: a preserved eclogite boudin (GR5) and a pervasively LP re-equilibrated micaschist (GR3), in order to reconstruct the entire [redacted] trajectory during the exhumation.

On the basis of micro-structural relationships and mineral chemistry data four Alpine metamorphic stages have been distinguished (Fig. 4): i) the peak-pressure metamorphic event (M1); ii) a first decompressional event (M2) [redacted] and iii) the tectono-metamorphic event (M3) responsible for the development of the main regional foliation under upper greenschist to amphibolite facies [redacted] Finally, a static re-equilibration occurred under amphibolite facies conditions (M4).

Minerals were analyzed with a Cambridge Stereoscan 360 SEM equipped with an EDS Energy 200 and a Pentafet detector (Oxford Instruments). The operating conditions were 15 kV accelerating voltage and 60 s counting time. Mineral formulae were recalculated assuming all measured FeO as [redacted] ept for clino-pyroxenes and amphiboles, for which [redacted] re calculated according to Linsdley and Anderson (1983) and according to the IMA-97 (Leake *et al.*, 1997) recommendation, respectively. Garnet [redacted] alculated on the basis of 12 oxygens, white mica on the basis of 11 oxygens, feldspar on the basis of 8 oxygens, chlorite on the basis of 28 oxygens, and epidote on the basis of 25 oxygens and assuming [redacted] = 1.1119*FeO. Representative mineral compositions of the selected samples are given in Tables 1 and 2. Abbreviations of minerals are given according to Kretz (1983) with the update of Bucher and Frey (2002).

4.1. Monte Rosa metabasites

The metabasites hosted within the garnet-micaschists of the Monte Rosa Nappe show different dimension from 10 cm to 5 m length and are represented by boudins enveloped by the S_1 regional foliation in the micaschists (Fig. 3a). Often, these boudins are good shear sense indicators and generally preserve a [redacted] foliation (pre-S1) (Fig. 5a) defined by eclogite facies assemblages (M1 assemblage: Omp + Grt + Phe + Gln + Qtz + Rt). Eclogites are partly re-equilibrated and developed a foliation defined by Cam (blue-green) + Chl + Bt + Wm + Ab + Spn + Qtz (M3 assemblage).

4.1.1. Sample GR5

Sample GR5 is a fine-grained eclogite with a spaced pre-S_1 foliation defined by elongated aggregates of Rt and by the PDO (Preferred Dimensional Orientation) of Phe (Fig. 5a). The M1 assemblage consists of Grt + Omp + Phe + Lws ([redacted] + Rt ± Gln ± Qtz and is partly overprinted by the M2 event characterized by the growth of Gln with up to 1 mm length at the expense of Omp (Fig. 5a) and by rare [redacted] (Figs. 5b). Zoisite grains are coarse grained (500 μm) and have inclusions of Grt + Omp (Fig. 5c) suggesting that it grew after the M1 assemblage. Further re-equilibration during decompression is testified by the growth of barroisite (Barr) rim around Gln at the expense of Omp (Figs. 5d), suggesting that Barr developed during the M2 event (Barr + Zo + Pg). The last re-equilibration stage consist of Czo/Ep neoblasts on Zo (Fig. 5c), rare Ab at the expense of Phe and Spn around Rt (M3 event: Czo/Ep + Ab + Spn).

Garnet

Garnet crystals show max 200 µm dimensions and have inclusions (max 25 µm in size; Fig. 5e) of abundant Omp + Qtz + Barr + Czo/Ep and rare Gln + Phe + Pg + Chl probably representing in part a relic prograde assemblage. Grt is zoned from core to rim with rather constant Alm, increasing Prp, decreasing Sps and first increasing and then decreasing Grs content. Thus, three different composition can be distinguished (Fig. 6a): the core with $Alm_{56-61}Grs_{29-33}Prp_{4-6}Sps_{4-8}$ composition, the mantle with $Alm_{56-59}Grs_{35-38}Prp_{5-6}Sps_{0-1}$ composition and finally the rim with $Alm_{57-61}Grs_{27-31}Prp_{10-12}Sps_{0-1}$ composition.

Omphacite

Omphacite is fine grained (max 100 µm) and is generally recrystallized in sub-grains. It shows slightly increasing Jd content from core (0.38-0.40) to rim (0.46-0.49) (Figs. 5f and 6b) and locally preserves relic cores with lower Jd content (min X_{Jd} 0.26). $X_{Mg}(Fe^{2+})$ is rather constant between 0.77-0.87 (X_{Mg} is 0.74-0.84 assuming all Fe^{2+}) without any correlation with X_{Jd}, while the Acm content is homogeneous and lower than 5 mol. %. Omp is also included in the Grt mantle and rim (Fig. 5e) and shows the same composition as the omphacite in the rock matrix (0.33-0.45 X_{Jd}; 0.70-0.78 X_{Mg} assuming all [redacted]

White mica

White mica has 250-300 µm dimensions and consists mainly of oriented phengite which defines a relict foliation and of rare Pg always associated to Zo. Phe shows decreasing Si content (Fig. 6c) from core (max 3.65 Si a.p.f.u.) to rim (min 3.31 Si a.p.f.u.). The zoning of phengite is not continuous showing a gap between 3.49-3.53 Si a.p.f.u. X_{Mg} decreases from core (0.82-0.88) to rim (0.64-0.68) while X_{Na} increases towards the rim up to 0.11.

Amphibole

Amphibole consists of a blue Gln core/mantle with a thin rim (50-100 µm thick) of green Barr (Fig. 6d). It has up to 1 mm length and shows PDO defining the relict foliation (pre-S_1), however its dimensions and the textural relationships with Grt and Omp suggest that Gln continues to grow after the relict foliation mainly at the expense of Omp. Gln has the composition 0.00-0.20

Al[IV] a.p.f.u., 1.65-1.80 Al[VI] a.p.f.u., 1.60-1.75 Na[B] a.p.f.u., 0.00-0.10 Na[A] a.p.f.u. with decreasing XMg from core (0.77-0.80) towards the Gln rim (0.64-0.67). The Barr rim is slightly zoned towards the outer rim, with increasing Al[IV] (from 0.55 to 0.95 a.p.f.u.), rather constant Al[VI] (0.95-1.15 a.p.f.u) and Na[B] (0.55-0.75 a.p.f.u.), increasing Na[A] (from 0.30 to 0.49 a.p.f.u. with up to 0.07 K[A] a.p.f.u.;) and decreasing XMg from 0.70 to 0.60. Locally the rim of Barr shows [Na + K]A ≥ 0.50 and is edenite/katophorite in composition (Fig. 6d), but this classification strongly depends on the assumption that all measured FeO was ferrous. The interface between Gln and Barr is very irregular (Fig. 5d) indicating that Gln, after being grown along the HP foliation, was resorbed before the growth of the Ca-Amph. Amphibole shows inclusions of Grt which is partially resorbed when in contact both with Gln and Barr (Fig. 5d) suggesting that Gln rim was not in equilibrium with the Grt rim and that Gln grew again after the M1 assemblage. Barr mainly grew at the expense of Omp + Gln + Grt.

Epidote

Epidote is in low amount and can be texturally distinguished into three generations: the first is included in Grt and has 0.14-0.45 [redacted] a.p.f.u. and is interpreted as a prograde relic (Zo); the second is coarser and sub-idiomorphic with low birefringence (Zo with less than 0.19 [redacted] a.p.f.u.) and grew in aggregates with Pg, the third (Clzo) shows higher birefringence, is idiomorphic and small grained and grows at the expense of Zo. The third generation is zoned showing increasing Fe3+ from core to rim (0.33-0.54 [redacted] a.p.f.u.).

4.2. Monte Rosa metapelites

The Alpine metamorphic evolution of the Monte Rosa metapelites is mainly characterized by two metamorphic events representing the development of the main regional foliation S_1 (M3 event) and a late re-equilibration developed under static conditions (M4 event) respectively. The S_1 regional foliation is defined by the M3 assemblage Phe + Pg + Grt II+ ChlI + Ab/Olig + Qtz + Rt/Ilm while the late static assemblage M4 consists of Ms + Pg + ChlII + Olig + Qtz + Bt + Ilm (Fig. [redacted]Furthermore, in the study area a few samples preserved a pre-S_1 foliation probably related to the HP metamorphism because of the high Si a.p.f.u. content of the relict phengite cores.

A representative [redacted] evaluate the metamorphic evolution of the southern side of the Monte Rosa Nappe in the Gressoney Valley. The sample shows a well developed S_1 foliation, [redacted]

[redacted]

4.2.1. Sample GR3

Sample GR3 is a medium to coarse-grained micaschist characterized by the bimodal distribution of garnet. The coarse-grained garnet (GrtI) is xenomorphic, has up to 3 mm dimensions and is partly enveloped by the main foliation (S_1), while the matrix garnet (GrtII) shows smaller dimensions (1-1.5 mm in diameter) and is in textural equilibrium with the minerals defining the regional foliation (S_1). A pre-S_1 foliation (Fig.7a) is preserved within isoclinal to rootless fold hinges and is defined by Phe + Pg + Rt. The high Si content of phengite cores suggest that pre-S_1 could represent an HP foliation, associated to the M1-M2 metamorphic stages.

The regional foliation S_1 is defined by Phe + Pg + GrtII + ChlI + Ab/Olig + Qtz + Rt/Ilm (M3 assemblage) and is partially overprinted by a late static assemblage M4 consisting of Olig + Ilm + ChlII + Ms + Pg + Qtz + Ilm. The presence of rare Hbl partially replaced by fine grained Chl + Qtz ± Olig aggregates along the S_1 foliation (Fig. 7b) is interpreted as part of a previous assemblage (M2).

Garnet

Garnet occurs as multistage xenomorphic coarse grains (GrtI) with up to 3 mm dimensions and as widespread idiomorphic grains with max 1-1.5 mm in diameter (GrtII). The coarse garnet preserves a [redacted] core showing fractures filled by a Grs-rich garnet (indicated by white arrows in Fig. 7c). GrtI is overgrown by a new garnet generation (GrtII) grown as smaller grains in the rock matrix (Fig. 7c). GrtI is unzoned with the $Alm_{80-85}Grs_{2-4}Prp_{7-9}Sps_{4-8}$ composition, while the fractures are filled by a grossular rich garnet with $Alm_{66-69}Grs_{18-23}Prp_{4-6}Sps_{6-8}$ composition. GrtII instead is slightly zoned (Fig. 8a-b-c) with the $Alm_{69-76}Grs_{13-19}Prp_{4-6}Sps_{5-6}$ composition at the core (similar to the garnet filling the fractures of GrtI), the $Alm_{79-81}Grs_{7-10}Prp_{9-11}Sps_{1-3}$ composition at the mantle and the $Alm_{77-80}Grs_{3-4}Prp_{16-19}$ composition at the rim. XMg increases from core (0.07-0.08) to rim (0.16-0.18). GrtI shows inclusions of Qtz, while GrtII includes Qtz, Rt and locally Rt rimmed by Ilm.

White mica

White mica consists of Phe and minor Pg which define the main foliation S_1 and the relict foliation pre-S_1. Phe is zoned with decreasing Si content (Fig 8d) from core (max 3.46 a.p.f.u) to rim (3.28-3.30 Si a.p.f.u.), with up 0.06-0.12 Na a.p.f.u. XMg does not show a good correlation with the Si content probably because of the presence of small amount of Fe^{3+} and roughly decreases from 0.75 to 0.63. The rim of Phe is overgrown by a late generation of white mica represented by Ms with 3.14-3.23 Si a.p.f.u and an XMg of 0.52-0.62 (Fig. 8d). Both phengite and paragonite show small inclusions of rutile.

Other minerals

Two generations of chlorite can be texturally distinguished: ChlI is medium-grained and is in lenses along the S_1 foliation while ChlII is fine-grained and is associated to Qtz or overgrew ChlI. ChlII + Qtz aggregates are interpreted as pseudomorphs after hornblende (Fig. 7d-e-f). Both ChlI and ChlII [redacted] (Fig. 8e). Both generations locally show fine grained Bt interlayer along the cleavage but it was not possible to acquire quantitative analyses because of its small dimensions. Plagioclase consists mainly of oligoclase with up to 0.25 XAn which locally preserve an albite core. Plagioclase locally shows a PDO defining the S_1 foliation and the rim instead grew after Phe, suggesting it is stable both during M3 and M4; ilmenite grew at the expense of Rt and has up to 1 wt. % of MnO.

Hornblende (Figs. 7e-f and 8f) is partly preserved and has 0.70-1.45 $Al^{[IV]}$ a.p.f.u. 0.85-1.10 $Al^{[VI]}$ a.p.f.u, and 0.15-0.40 $Na^{[B]}$ a.p.f.u., 0.12-0.42 $Na^{[A]}$ a.p.f.u. and 0.51-0.62 XMg, and is replaced by Qtz + Chl (0.49-0.51 XMg) ± Olig (0.72-0.74 XAb). .

5. [redacted]

Metamorphic conditions for the polymetamorphic Complex of the Monte Rosa Nappe in the Gressoney-Ayas Valleys have been reconstructed [redacted] of the eclogite (GR5) and the metapelite (GR3) samples described above. All pseudosections have been calculated with PERPLE_X (Connolly, 1990; Connolly and Petrini, 2002) using the thermodynamic database of Holland and Powell (1998, 2004 upgrade).

All pseudosections have been calculated assuming all FeO as ferrous, and H_2O saturated conditions with a pure H_2O fluid-phase (aH_2O = 1). This is a realistic assumption for the studied samples since they contains abundant hydrous phases and because of the absence of primary carbonates and sulphurs. The following solid solution models have been used: [redacted] [redacted] clino-pyroxene (Green *et al.*, 2007), amphibole (Dale *et al.*, 20[illegible], feldspar (Holland and Powell, 2003; or Furman and Lindsley, 1988), paragonite ([redacted] and Froese, 1975), phengite-muscovite (Holland, 2002), chlorite, chloritoid, staurolite and carpholite (Holland and Powell, 1996, [redacted]

[redacted] In all pseudosections, [redacted] and small letters indicate pure phases. All calculated pseudosections consist of di-, tree-, quadri-, penta-, six-variant fields which are represented in white (di-variant) and with progressively darker grey hues.

The bulk rock composition for the studied samples (Table 3) has been established by the XRF method at the Vancouver laboratories of the ALS Chemex. The location of the studied samples is reported in Fig. 2.

5.1 Results for pseudosection modelling of GR5 (eclogite)

The M1 assemblage (Grt + Omp + Phe + Qtz + Lws + Rt ± Gln) represent the peak-pressure event and was modelled in the PT range of 13-29 kbar and of 350-700 °C with [redacted] Two pseudosections were calculated, the first (I) with SiO2 saturated conditions as justified by the presence of Qtz inclusions in Grt and the second (II) with SiO_2 saturated conditions and constraining [redacted] according to the measured Gln composition.

In pseudosection I (Fig. 9a) the Grt compositional isopleths cross only at the Grt rim in the Omp + Grt + Tlc + Phe + Lws + Qtz ± Gln at 555-565 °C and 25-27 kbar (Fig. 9b). No Tlc was observed in the sample and the reason for the unmatched composition for garnet core and mantle could be the SiO2-H2O saturated conditions or the modelled composition of Gln which is too Fe-rich (0.15-0.55 XMg; Fig. 9c) relative to the XMg measured (0.65-0.80). The SiO_2 saturation condition is constrained by abundant Qtz inclusions in garnet and by low amount of Qtz in the matrix. Since the H_2O content in the rock at the PT conditions of Grt rim (1.0-3.0 wt. %; Fig. 9d) is a reasonable one and since the compositional discrepancy between calculated and modelled Gln is very large, pseudosection II was calculated constraining the XMg of Gln to values ≥ 0.60.

Pseudosection II (Fig. 10a) is contoured for Alm-Grs-Prp isopleths from garnet core ($Alm_{56-61}Grs_{29-33}Prp_{4-6}$) to rim ($Alm_{57-61}Grs_{27-32}Prp_{10-12}$) compositions (Fig. 10b), for XJd and XMg in omphacite (Fig. 10c), for Si a.p.f.u. in phengite and for $Na^{[B]}$, $Al^{[IV]}$ and XMg in Ca-amphibole (Fig.

10d). The garnet core isopleths cross at 495-525 °C and 21-24 kbar and the rim at 550-570 °C and 24-27 kbar. Along this path (black arrow in Fig. 10b) the sequence of the metamorphic assemblages is Gln + Lws, Cam + Gln + Lws, Tlc + Cam + Gln + Lws, Tlc + Gln + Lws, Tlc + Lws (with Grt + Omp + Phe + Qtz in excess). [redacted]

Along the inferred PT path, the Grt core is in equilibrium with a Di-rich Cpx (0.15-0.25 XJd) which is quickly replaced or overgrown by a Jd- rich Omp (0.30-0.45 XJd) in equilibrium with the garnet rim (Fig. 10c). Therefore along this path garnet was in equilibrium with omphacite showing 0.15-0.45 XJd and XMg 0.55-0.75 (Fig. 10c), and phengite with max 3.70 Si a.p.f.u. (Fig. 10c). The calculated compositions agree with the measured one except for the presence of a Jd poor pyroxene generation (XJd < 0.25) with an intermediate XMg value (0.55-0.60) which has not been observed and which was probably resorbed during the growth of Omp. The max XJd and XMg in the Na-Ca pyroxene are reached during a first decompression stage (XJd = 0.46 and XMg = 0.80-0.81) at 575-600 °C and 21-22 kbar in the Omp + Grt + Phe + Cam + Qtz ± Gln stability field (black arrow in Fig. 10c).

The path A [redacted] a near-isothermal decompression trough the Gln stability field towards the Barr stability field, while path B represents a decompressional heating outside of the Gln stability field. Path A better represents textural relationships observed in the studied sample as Gln continued to grow after the M1 assemblage and then was resorbed before Barr growth. In the calculated pseudosection (Fig. 10), Barr should be in equilibrium with Omp (XJd 0.45-0.46; XMg 0.60-0.70) while in our sample Barr grew at the rim of Gln and at the expense of Omp (XJd 0.46-0.49; XMg 0.75-0.84).

The second decompression step is constrained by the composition of Barr (0.55-0.95 $Al^{[IV]}$; 0.55-0.75 $Na^{[B]}$; 0.60-0.70 XMg) and by the Si content of the Phe rim (min 3.30 Si a.p.f.u.) and developed at 580-630 °C and 14.5-16.5 kbar in the Grt + Omp + Phe + Cam + Zo + Qtz stability field (Fig. 10d).

All the previous observations and because of the great uncertainties in the amphibole solution model suggest that the PT conditions inferred for the exhumation path have to be treated with caution.

[redacted]

[redacted] The garnet rim contours cross at 550-565 °C and 23.5-26 kbar mainly in the Grt + Omp + Phe + Tlc + lws + Qtz ± Tlc field at slightly lower P compared to the unfractionated composition. The Tlc amount in equilibrium with the Grt rim (Fig. 10f) is 7-9 vol. % and the Omp composition shows 0.47 XJd and 0.80-0.82 XMg on decompression similarly to Fig. 10c. This mean that the change in the effective bulk composition reacting during prograde metamorphism does not influence as much the minerals composition.

5.2. Results for pseudosection modelling of GR3 (metapelite)

5.2.1. PT conditions for GrtI generation

GrtI generation represent the relic of a metamorphic event older than the M3 assemblage. Since there is no other relic mineral and the only inclusions in GrtI consist of Qtz + Ilm, the PT condition of equilibration for GrtI are poorly constrained and are only based according to its composition ($Alm_{80-86}Grs_{2-5}Prp_{7-9}$). In the pseudosection of Fig. 11 no intersection has been identified at high pressure, therefore GrtI cannot be related to the Alpine eclogite facies event (M1/M2 assemblages) as already suggested by Ilm inclusions. Instead, the GrtI isopleths intersect at 550-575 °C and 4-6 kbar conditions in the Bt + Chl + Grt + Pl + Phe (Ms) + Qtz ± Pg ± St field. Therefore, GrtI generation can be considered as a pre-Alpine relic belonging to the Variscan orogenesis. These PT conditions are a minimum estimation of the pre-Alpine event since GrtI is strongly resorbed and fractured.

5.2.2. PT conditions for GrtII generation

The M3 (Phe + Pg + Grt II + ChlI + Ab/Olig + Qtz) and M4 assemblages (Ms + Pg + ChlII + Olig + Qtz + Bt) were modelled in the PT window 5-15 kbar and 500-650 °C with Qtz + Ms/Phe in excess (Fig. 12a). Since the Gln has revealed a problem in pseudosection modelling of sample GR5 and since there is no evidence of former presence of this mineral in this sample where the only amphibole is relict Hbl, the Gln and Act solution models were rejected from calculations. This means that the HP portion of the pseudosection could be metastable relative to Gln. The relative bulk rock composition (2.98 MnO, 1.03 CaO, 37.24 FeO, 2.02 MgO, 20.21 Al_2O_3, [redacted] in wt. %) has been calculated, according to the method of Gaidies *et al.* (2006), fractionati[illegible]2 vol. % of the average composition of GrtI.

The pseudosection is contoured for Alm, Grs, Prp isopleths for the GrtII core ($Alm_{69-76}Grs_{12-18}Prp_{5-7}$) (Fig. 12b), mantle ($Alm_{79-81}Grs_{7-10}Prp_{9-11}$) and rim ($Alm_{77-80}Grs_{3-4}Prp_{16-19}$) compositions (Fig. 12c); while in Fig 12d the Si isopleths in phengite, XMg in chlorite and XAn in plagioclase are reported. The resulting PT path according to the garnet growth zoning represented by GrtII core to mantle compositional zoning, suggests a near isobaric prograde event from 550 to 600 °C at 6.5-7.5 kbar (Fig. 12d) within the Bt stability field. In particular, the mantle composition of GrtII is stable with Bt (max 3-4 vol. %) + Chl (XMg 0.46-0.52) + Pl (XAn < 0.30) + Ms (3.15-3.10 Si a.p.f.u.) + Pg + Qtz.

[redacted] Indeed, the fractionation of Si-rich Phe could displace the Bt-in towards higher T or could reduce its vol. % amount. GrtII rim should be stable with 4-5 vol. % St, with up to 11-14 % Bt, with andesine (XAn > 0.30) and in absence of Chl. In this case all the Chl should be interpreted as pseudomorph after St + Bt but since ChlI define the regional foliation it seems unlikely. However, we cannot exclude that ChlII represents pseudomorphs after former Bt during retrogression. The absence of obvious pseudomorphs after St together with the XMg of Chl (0.46-0.52) constrain the maximum PT conditions for the M3 event at *ca* 600 °C and 7.5 kbar where the rock should contain less than 4 vol. % of Bt.

In this case, the GrtII rim composition does not reflect M3 peak conditions. This should be related to a later diffusion process and the M3 event should represent a re-heating of max 40 °C during the development of the regional foliation, while the M4 event developed immediately after the peak T during retrogression as suggested by the composition of ChlII which developed also at the expense of GrtII.

Finally, the presence of Hbl partially destabilizated in Chl + Qtz ± Olig (see Figs. 7e-f) is compatible with the dashed decompressional path reported in Fig. 12d and should represent a pre-S_1 relic phase related to the M2 decompressional assemblage.

Another pseudosection for GR3 metapelite was calculated using the feldspar solution model of Furman and Lindsley (1988) to check the difference with the Holland and Powell (2003) model which slightly seems to overestimate the Ca content in plagioclase. The use of this solution model changes the pseudosection topology shifting the Bt-in reaction towards higher T (compare Figs. 12a and 13a). The intersection of Grt contours for the core composition constrain its stability at 545-555 °C and 7-7.5 kbar in the biotite-out stability field (Fig. 13b). The GrtII mantle contours cross at 580-595 °C and 8.5-9 kbar always in the Chl + Phe + Pg + Pl + Grt + Qtz field assemblage, while the rim should be in equilibrium also with Bt (max 3 vol. %) at 610-620 °C and 8.5-9 kbar (Fig.

13c). If the ChlII should be partly interpreted as pseudomorph after former Bt during retrogression these PT conditions are likely, otherwise the Tmax in constrained to *ca* 590°C by the Chl composition. The resulting PT path differs from the previous one because the prograde trajectory is slightly compressional instead of isobaric.

The use of different feldspar solution model does not change as much the PT conditions for the M3 assemblage and the contours intersection of garnet and chlorite but the Furman and Lindsley (1988**)** model justifies in a better way the equilibrium assemblage identified in this sample and the plagioclase composition, probably also because the CaO content in the rock composition is very low (0.30 wt.%).

6. Discussion

In Fig. 14 the complete Alpine P–T path inferred for the southern side of the Monte Rosa Nappe in the Gressoney valley is reported. All the curves representing the geothermal gradients were calculated assuming an average density of 2.95 kg/dm^3 for an heterogeneous subducted crust for P > 10 kbar (Bousquet *et al.*, 1997). At lower P where the average density is less (2.70-2.80 kg/dm^3) the curves lay at slightly lower pressures without significant changes because of the close spacing of the geothermal gradients.

[redacted]

The eclogitic boudins on the south western part of the Monte Rosa Nappe registered peak pressure conditions which occurred at 550-570 °C and 24-27 kbar and are characterized by the assemblage Omp + Grt + Lws + Phe + Qtz + Gln + Rt ± Tlc (inferred from pseudesection modelling) while the only HP relic found in metapelites is Phe with high Si content (3.45-3.50 a.p.f.u.). The inferred PT conditions for the M1 event are similar to previous estimations on whiteschists which yield 505 ± 30 °C and 24 kbar (Le Bayon *et al.*, 2006) while P is significantly higher compared to values reported in the southern part of the nappe by Chopin & Monié (1984) (17 kbar and 500 °C), Dal Piaz and Lombardo, (1986) and Borghi *et al.*, (1996) (10 ± 2 kbar and 500 ± 50 °C) and by Lapen *et al.* (2007) in the Furgg Zone (P > 13 kbar and 480-570 °C). [redacted]n the T value is appreciably higher (ca 60°) than those reported in literature and similar to that recently inferred for the HP event in the Gran Paradiso Massif (Gabudianu et al., 2009; Gasco et al., 2010).

The M2 metamorphic stage consists of the assemblage Omp + Grt + Amph + Zo + Phe + Pg + Qtz + Rt in the eclogites. This event can be divided in two successive decompressional stages. The first developed in the Gln-Cam stability field at 575 – 600 °C and 21-22 kbar, wile the second step occurred at 590-630 °C and 14.5-16.5 kbar suggesting a T increase during decompression. The presence of this heating stage during decompression at still HP conditions is mainly related to the amphibole composition: being aware of the many uncertainties in this solution model (Dale *et al.*, 2005), these PT conditions have to be treated with caution. If these PT conditions of re-equilibration at HP were true, the garnet and omphacite preserved in the rock are metastable in composition relative to Barr. However, similar rocks were studied by Zhang *et al.*, (2009) in the Western Dabie Mountain (Central China) and the PT path reconstructed for the Monte Rosa eclogites is very similar to that proposed by these authors. The presence or absence of this decompressional heating (Fig. 14) does not influence the average exhumation rates but clearly have different meanings: indeed such an heating event at a depth of 50-60 km during exhumation could be linked to the slab breakoff model (Davies and Von Blanckenburg, 1995) and to the ascent of astenospheric mantle and could explain the almost complete overprinting of the M1 assemblage in the metapelites. Taking into account the inaccuracy of the amphibole solution model and supposing that Barr represent a local equilibrium, an alternative post-peak trajectory is represented by the dashed line of Fig. 14.

The subsequent M3 tectono-metamorphic event developed syn-kinematically respect to the main regional foliation S_1 and is characterized by the assemblage Phe + Pg + Grt + Chl + Ab/Olig + Hbl + Qtz + Ilm in metapelites and by Cam (blue-green) + Chl + Ab + Bt + Qtz + Pg + Phe +Clzo in the re-equilibrated metabasite boudins. It developed during increasing T from 550 to ca. 600°C at 7 - 9 kbar. The maximum T reached depends mainly on the interpretation of the Chl (see Fig 13). If Chl can be partly interpreted as pseudomorph after Bt the maximum T reached is [redacted] otherwise is 590° C. Since in the studied metapelites Bt is present in low amoun[illegible]he first hypothesis is more reliable. These PT estimation are different from that of Le Bayon *et al.* (2006) who reported for the decompressional event associated to the regional foliation in the whiteschists T of 475 ± 30 °C and P of 8 kbar. Other PT data for the retrograde event are reported for the central eastern portion of the Monte Rosa Nappe where rocks reached T range from 580 to 750 °C at 9-12 kbar (Engi *et al.*, 2001).

7. Conclusions

The pseudosection modelling of two chemical systems (both metabasites and metapelites) allowed to reconstruct a portion of the PT path followed by the southern Monte Rosa Nappe during the Alpine orogenesis (Upper Gressoney Valley). In particular, well preserved eclogite facies rocks (M1 and M2 assemblages) were investigated to reconstruct the HP history related to the subduction event, while re-equilibrated metapelites allowed to infer the PT conditions attained during the development of the exhumation regional foliation (M3 to M4 assemblages). The metamorphic evolution of the basement complex from the Monte Rosa Nappe is marked by texturally distinct mineral assemblages, defining four Alpine metamorphic stages (M1, M2, M3 and M4) developed under different PT conditions. The M1 and M3 tectono-metamorphic stages are related to the development of the pre-S_1 and S_1 foliations, respectively.

The reconstructed PT path (Fig. 14) shows a clockwise trajectory characterized by a prograde stage along a 6-7 °C/km geothermal gradient up to the eclogitic peak pressure (M1 stage). The exhumation path is linked to a slightly decompressional heating (ca. 40 °C and 10 kbar) up to the development of the second stage of the M2 metamorphic event. Further exhumation is accompanied to cooling down to 540-550 °C and 7-9 kbar implying an exhumation of 25 km (7-8 kbar) linked to a T decrease. Afterwards, rocks followed a slightly compressional (from 7 to 9 kbar) trajectory associated to an increase in T (from 550 to 600 °C) accompanied to the development of the main regional foliation. During this event the apparent geothermal gradient range between 15 and 20 °C/km. Further exhumation was related to major cooling up to shallow crustal levels.

[redacted] In Fig. 14 is also reported the trajectory proposed by Borghi *et al.*, (1996). It shows similar shape respect to inferred path presented in this work, bat placed at lower P-T conditions. [redacted]

Moreover, the reconstructed trajectory is marked by a late thermal pulse accompanied by a limited burial stage. Recently, evidence of burial–exhumation cycles that took place during a single orogeny have been reported by Beltrando *et al.* (2007) in the Piedmont Zone, in the area located between the Gran Paradiso massif and the Aosta Valley. Based on geochronological data reported in literature, the HP stage has been dated at 42-43 Ma by Lapen *et al.* (2007) while the re-equilibration stage range from 32 to 38 Ma (Engi *et al.*, 2001) in the central to eastern Monte Rosa. [redacted]

[redacted]

Acknowledgments

We are grateful to J.A.D. Connolly (ETH, Zurich) for the useful suggestions during pseudosections modelling. This work was financially supported by Ministero dell'Università e della Ricerca Scientifica e Tecnologica (M.U.R.S.T.).

References

Bearth, P., 1952. Geologie und Petrographie des Monte Rosa. Beiträge Geologische Karte Schweiz, Neue Folge 96, 1–94.

Bearth, P., 1954. Geologischer Atlas der Schweiz 1 :25.000, Blatt Saas Nr. 30. Schweizerische Geologische Kommission.

Beltrando, M., Lister, G.S., Hermann, J., Forster, M., Compagnoni, R., 2008. Deformation mode switches in the Penninic units of the Urtier Valley Western Alps: evidence for a dynamic orogen. Journal of Structural Geology, 30, 194–219.

Borghi, A., Compagnoni, R., Sandrone, R. 1996. Composite P-T paths in the internal Penninic massifs of the western Alps: Petrological constrains to their thermo-mechanical evolution. Eclogae Geologicae Helvetiae, 89, 345–367.

Bousquet, R., Goffé, B., Henry, P., Le Pichon, X., Chopin, C. 1997. Kinematic, thermal and petrological model of the Central Alps : Lepontine metamorphism in the upper crust and eclogitisation in the lower crust. Tectonophysics, 273, 105-127.

Bucher, K., Frey, M., 2002. Petrogenesis of Metamorphic Rocks. Springer-Verlag, 7th edition, p. 335-336

Bucher S., Schmid S.M., Bousquet, R., Fügenschuh, B., 2003. Late stage deformation in a collisional orogen Western Alps: nappe refolding, back thrusting or normal faulting? Terra Nova, 15, 109-117.

Castelli, D., Rolfo, F., Groppo, C., Compagnoni, R., 2007. Impure marbles from the UHP Brossasco-Isasca Unit Dora-Maira Massif, western Alps: evidence for Alpine equilibration in the diamond stability field and evaluation of the XCO2 fluid evolution. Journal of Metamorphic Geology, 25, 587-603

Chatterjee, N.D., Froese, E., 1975. A thermodynamic study of the pseudobinary join muscovite-paragonite in the system KAlSi3O8–NaAlSi3O8–Al2O3–SiO2–H2O. American Mineralogist, 60, 985-993.

Connolly, J.A.D., 1990. Multivariable phase diagrams: an algorithm based on generalized thermodynamics. American Journal of Science, 290, 666-718.

Connolly J.A.D., Petrini K., 2002. An automated strategy for calculation of phase diagram sections and retrieval of rock properties as a function of physical conditions. Journal of Metamorphic Geology, 20, 697-708.

Chopin, C., 1984. Coesite and pure pyrope in high-grade blueschist of the Western Alps: a first record and some consequences. Contributions to Mineralogy and Petrology, 86, 107-118.

Chopin, C., Monié, P., 1984. A unique magnesiochloritoid – bearing high pressure assemblage from the Monte Rosa, Western Alps: petrologic and ^{40}Ar – ^{39}Ar radiometric study. Contribution to Mineralogy and Petrology, 87, 388-398.

Chopin, C., Henry, C., Michard, A., 1991. Geology and petrology of the coesite-bearing terrain, Dora Maira massif, Western Alps. European Journal of Mineralogy, 3, 263– 291.

Dale, J., Powell, R., White, R.W., Elmer, F.L., Holland, T.J.B., 2005. A thermodynamic model for Ca–Na clinoamphiboles in Na2O–CaO–FeO–MgO–Al2O3–SiO2–H2O–O for petrological calculations. Journal of Metamorphic Geology, 23, 771-791.

Dal Piaz, G.V., 1964. Il cristallino antico del versante meridionale del Monte Rosa, paraderivati a prevalente metamorfismo alpino. Rendiconti della Società Mineralogica Italiana, 20, 101-135

Dal Piaz, G.V., 1966. Gneiss ghiandoni, marmi ed anfiboliti antiche del ricoprimento Monte Rosa nell'alta Valle d'Ayas. Bollettino della Società Geologica Italiana, 85, 103-132.

Dal Piaz, G.V. 1971. Nuovi ritrovamenti di cianite alpina nel cristallino antico del Monte Rosa. Rend. Soc. It. Miner. Petrol., 27, 437.477.

Dal Piaz, G.V., 2001. Geology of the Monte Rosa Massif: historical review and personal comments. Schweizerische Mineralogische und Petrographische Mitteilungen, 81, 275-303.

Dal Piaz G.V., Lombardo, B,. 1986. Early_alpine eclogite metamorphism in the Penninic Monte Rosa-Gran Paradiso basement nappes of the north-western Alps. Geological Society of America Memoirs, 164, 249-265.

Davies, J.H., Von Blanckenburg, F., 1995. Slab breakoff: a model of lithosphere detachment and its test in the magmatism and deformation of collisional orogens. Earth and Planetary Sciences Letters, 129, 85-102.

Engi, M., Scherrer, N.C., Burri T., 2001. Metamorphic evolution of pelitic rocks of the Monte Rosa Nappe: Constrains from petrology and single grain monazite age data. Schweizerische Mineralogische und Petrographische Mitteilungen, 81, 305–328.

Escher, A., Hunziker, J.C., Marthaler, M., Masson, H., Sartori, M., Steck, A., 1997. Geologic framework and structural evolution of the western Swiss-Italien Alps. In: Pfeiffner, O.A., Lehner, P., Heitzmann, P.,Müller, S., Steck ,A. Eds.: Deep Structure of the Alps, Results of NRP 20. Birkhäuser. Basel Boston Berlin, 205–222.

Evans T.P, 2004. A method for calculating effective bulk composition modification due to crystal fractionation in garnet-bearing schist: implications for isopleth thermobarometry. Journal of Metamorphic Geology, 22, 547-557.

Ferrando, J., 2002 Evoluzione tettonica e metamorfica delle eclogiti incluse nella crosta continentale del Monte Rosa.Unpublished Thesis, Facoltà di. Science, University of Genova, Genova, Italy

Ferrando, J., Scambelluri, M., Dal Piaz, G.V., Piccardo, G.B.,2002. The mafic boudins of the southern Furgg-Zone, Monte Rosa Nappe, NW-Italy: from tholeiitic continental basalts to Alpine eclogites and retrogressed products. Abstr. 81a Riunione Estiva Società Geologica Italiana, Torino 10-12 September 2002.

Frey, M., Hunziker., J.C., O'Neil J.R., Schwander H.W., 1976. Equilibrium-disequilibrium relations in the Monte Rosa granite, western Alps: petrological, Rb-Sr and stable isotope data. Contributions to Mineralogy and Petrology, 55, 147-179.

Froitzheim, N., 2001. Origin of the Monte Rosa Nappe in the Pennine Alps – A new working hypothesis. GeologicalSociety of America Bulletin, 5, 604-614.

Furman, M.L., Lindsley, D.H., 1988. Ternary feldspar modeling and thermometry. American Mineralogist, 73, 201– 215

Gabudianu Radulescu, I., Rubatto, D., Courtney, G. Compagnoni, R., 2009, The age of HP metamorphism in the Gran Paradiso Massif, Western Alps: A petrological and geochronological study of "silvery micaschists", Lithos, 110, 95-108.

Gasco, I., Gattiglio, M., 2011. Geological map of the upper Gressoney Valley, Western Italian Alps. Journal of Maps, in press.

Gasco, I; Borghi, A; Gattiglio, M. 2010 Metamorphic evolution of the Gran Paradiso Massif: A case study of an eclogitic metagabbro and a polymetamorphic glaucophane–garnet micaschist. Lithos, 115, 101-120

Gasco, I, Gattiglio, M., Borghi, A., 2011. Lithostratigraphic setting and P-T metamorphic evolution for the Dora Maira Massif along the Piedmont Zone boundary middle Susa Valley, NW Alps Inter. J. Earth Scieces, in press.

Gaidies, F., Abart, R., De Capitani, C., Schuster, R., Connolly, J.A.D., Reusser E., 2006. Characterization of polymetamorphism in the Austroalpine basementa east of the Tauern Window using garnet isopleth thermobarometry. Journal of Metamorphic Geology, 24, 451-475.

Green, E.C.R., Holland, T.J.B., Powell, R., 2007. An order-disorder model for omphacitic pyroxenes in the system jadeite-diopside-hedenbergite-acmite, with applications to eclogite rocks. American Mineralogist, 92, 1181-1189.

Holland, T.J.B., Powell, R., 1996. Thermodynamics of order–disorder in minerals 2. Symmetric formalism applied to solid solutions. American Mineralogist 81,1425–1437.

Holland, T.J.B., Powell, R., 1998. An internally consistent thermodynamic data set for phases of petrologic interest. Journal of Metamorphic Geology 16, 309–343.

Holland, T.J.B., 2002. Index of solid solution model and internally consistent thermodynamic dataset. University of Cambridge, Department of Earth Sciences. From the T.J.B. Holland website http://www.esc.cam.ac.uk/astaff/holland/ds5/.

Holland, T.J.B., Powell, R., 2003. Activity–composition relations for phases in petrological calculations: an asymmetric multicomponent formulation. Contributions to Mineralogy and Petrology 145, 492–501.

Hunziker, J.C., 1970. Polymetamorphism in the Monte Rosa, Western Alps. Eclogae Geologicae Helvetiae, 63, 151-161.

Inger, S., Ramsbotham, W., 1997. Syn-convergent exhumation implied by progressive deformation and metamorphism in the Valle dell'Orco transect, NW Italian Alps. Journal of the Geological Society of London, 154, 667- 677.

Jaboyedoff, M., Béglé P., Lobrinus S., 1996. Stratigraphie et évolution structurale de la zone de Furgg, au front de la Nappe du Mont-Rose. Bulletin de la Société Vaudoise des Sciences Naturelles, 84/2, 191-210.

Keller, L.M., Schmid, S.M., 2001, On the kinematics of shearing near the top of the Monte Rosa Nappe and the nature of the Furgg zone in Val Loranco Antrona Valley, N. Italy: tectonometamorphic and paleogeographic consequences Schweizerische Mineralogische und Petrographische Mitteilungen, 81, 347–367.

Keller, L. M., Hess, M., Fügenschuh, B., Schmid, S. M., 2005. Structural and metamorphic evolution of the Camughera-Moncucco, Antrona and Monte Rosa units southwest of the Simplon line, Western Alps. Eclogae Geologicae Helvetiae, 98, 19-49.

Kramer, J., 2002 Structural evolution of the Penninic units in the Monet Rosa region Swiss and Italien Alps. PhD University of Basel, 154pp.

Kretz, R., 1983. Symbols for rock-forming minerals. American Mineralogist, 68, 277-279.

Lange S., Nasdala, L., Poller, U., Baumgartner, L.P., Todt, W., 2000. Crystallization age and metamorphism of the Monte Rosa Granite, Western Alps. Abstr. 17th Swiss Tectonic Studies Group Meeting, Zürich, p. 51.

Lapen, T.J., Johnson, C.M, Baumgartner, L.P., Dal Piaz, G.V., Skore, S., Beard, B., 2007. Coupling of oceanic and continental crust during Eocene eclogite-facies metamorphism: evidence from tha Monte Rosa Nappe, western Alps.Contributions to Mineralogy and Petrology, 153, 139-157.

Leake, B.E., Woolley, A.R., Arps, C.E.S., Birch, W.D., Gilbert, M.C., Grice, J.D., Hawthorne, F.C., Kato, A., Kisch, H.J., Krivovichev, V.G., Linthout, K., Laird, J., Mandarino, J.A., Maresch, W.V., Nickel, E.H., Rock, N.M.S.,Schumacher, J.C., Smith, D.C., Stephenson, N.C.N., Ungaretti, L., Whittaker, E.J.W., Guo, Y., 1997. Nomenclature of amphiboles; report of the subcommittee on amphiboles of the International Mineralogical Association, Commission on New Minerals and Mineral Names. Canadian Mineralogist, 35, 219-246.

Le Bayon, R., de Capitani, C., Chopin, C. Frey, M., 2000. Modelling of the sequential evolution of whiteschist assemblages: HP in the Monte Rosa Western Alps. Beihefte European Journal of Mineralogy, 12, 111.

Le Bayon, R., de Capitani, Frey R., 2006. Modelling phase–assemblage diagrams for magnesian metapelites in the system K2O–FeO–MgO–Al2O3–SiO2–H2O: geodynamic consequences for the Monte Rosa Nappe, Western Alps. Contributions to Mineralogy and Petrology, 151, 395-412.

Le Bayon, B., Pitra, P., Ballèvre, M., Bohn, M., 2006. Reconstructing P-T paths during continental collision using multi-stage garnet Gran Paradiso nappe, Western Alps. Journal of Metamorphic Geology, 24, 477-496.

Liati, A., Gebauer, D., Froitzheim, N., Fanning, M.C., 2001 U-Pb SHRIMP geochronolgy of an amphibolitized eclogite and an orthogneiss from the Furgg zone western Alps and implications for its geodynamic evolution. Schweizerische Mineralogische und Petrographische Mitteilungen, 81, 379–393

Lindsley, D.H., Anderson, D.J. 1983 A two-pyroxene thermometer. Journal of Geophysical Research, 88A, 887-906.

Marmo, B.A., Clarke, G.L., Powell, R., 2002. Fractionation of bulk rock composition due to porphyroblast growth; effects on eclogite facies mineral equilibria, Pam Peninsula, New Caledonia. Journal of Metamorphic Geology, 20, 151-165

Pawlig, S., Baumgartner, L.P., Hauzenberger, C.,A, 2001. Geochemistry of a talc-chloritoid-kyanite shear zone within the Monte Rosa granite, Val d'Ayas, Italy. Schweizerische Mineralogische und Petrographische Mitteilungen, 81, 329–346

Pleuger, J., Froitzheim, N., Jansen, E., 2005. Folded continental and oceanic nappes on the southern side of MontenRosa western Alps, Italy: Anatomy of a double collision suture. Tectonics, 24, TC4013, doi:10.1029/2004TC001737.

Pleuger, J., Roller, S., Walter, J.M., Jansen, E., Froitzheim, N., 2007. Structural evolution of the contact between two Penninic Nappes Zermatt-Saas zone and Combin zone, Western Alps and implications for the exhumation mechanism and palaeogeography. International Journal of Earth Sciences, 96, 229-252.

Pognante, U., Talarico, F., Rastelli, N., Ferrati, N., 1987. High pressure metamorphism in the nappes of the Valle dell'Orco traverse Western Alps collisional belt. Journal of Metamorphic Geology, 5, 397-414.

Reddy, S.M., Wheleer, J., Cliff, R.A., 1999. The geometry and timing of orogenic extension: an example from the Western Italian Alps. Journal of Metamorphic Geology, 17, 573-589.

Schmid, S.M., Fügenschuh, B., Kissling, E., Schuster, R., 2004. Tectonic map and overall architecture of the Alpine orogen. Eclogae Geologicae Helvetiae, 97, 93–117.

Steck, A., Biggioggero, B., Dal Piaz, G.B., Escher, A., Martinotti, G., Masson, H., 1999. Carte tectonique des Alpes de Suisse occidentale et des regions avoisinantes, carte gèologique spèciale, 123. Service hydrologique et gèologique national, Bern, Switzerland.

Stüwe, K., 1997. Effective bulk composition changes due to cooling: a model predicting complexities in retrograde reaction textures. Contributions to Mineralogy and Petrology, 129, 43–52.

Tajcmanova, L., Connolly, J.A.D., Cesare, B., 2009. A thermodynamic model for titanium and ferric iron solution in biotite. Journal of Metamorphic Geology, 27, 153-165.

White, R. W., Powell, R., Holland, T. J. B., 2007. Progress relating to calculation of partial melting equilibria for metapelites. Journal of Metamorphic Geology, 25, 511-527.

Zhang, J., Wei, C., Lou, Y., Su, X., 2009. Phase Equilibria of Hornblende-Bearing Eclogite in the Western Dabie Mountain, Central China. Acta Geologica Sinica-English Edition, 83, 57-69.

Figure captions

Fig. 1. a) Simplified tectonic map of the Western Italian Alps (modified after Schmid *et al.*, 2004). The black box is enlarged in b); b) simplified geological map of the Monte Rosa Massif and surrounding units (redrawn by Dal Piaz and Lombardo, 1986; Steck *et al.*, 1999; Pleuger *et al.*, 2005). The dashed box shows the study area on the south side of the Monte Rosa Massif.

Fig. 2. Simplified geological map of the study area showing the position of the studied samples. For a detailed geological map see Gasco and Gattiglio (2011).

Fig. 3. Main rock types of the study area: a) eclogite boudins within the garnet-micaschists; b) transitional contact marked by intercalations (black arrows) between garnet-micaschists and albite-micaschists just below the tectonic contact with the Zermatt-Saas metabasites; c) Bt + Grt rich dark

nodules in a light quartz-feldspatic matrix interpreted as meta-anatexites of pre-Alpine age; d) stretched meta-rodingites layers within the serpentinites.

Fig. 4. Mineral abundances and relationships between the metamorphic evolution and the deformation stages of the studied samples.

Fig. 5. Microstructures of sample GR5: a) well preserved eclogite with a pre-S_1 foliation mainly defined by PDO of Phe and of Rt aggregates. Omp is partly recrystallized in subgrains and Gln has up to 1 mm size and shows a Barr rim; b) Pg + Zo association overgrowing the pre-S_1 foliation interpreted as lozenge-shaped pseudomorph after Lws (highlighted by the red dotted line). Back-scattered images of eclogite GR5: c) Zo + Pg aggregate interpreted as pseudomorphs after Lws. Coarse Zo has inclusions of Grt + Omp and is overgrown by late Czo; d) Gln with a Barr rim overgrowing the M1 assemblage (mainly Grt + Omp). Barr also developed at the expense of Omp; e) Qtz + Czo/Ep + Barr + Omp inclusions in Grt; f) zoned Omp showing increasing Jd content from core (brighter) to rim (darker).

Fig. 6. Minerals chemistry of sample GR5. a) chemical zoning rim-to-rim profile of garnet; b) chemical composition of omphacite showing increasing Jd content from core to rim; c) composition of white micas showing decreasing Si content from core to rim; d) chemical composition of amphibole showing a glaucophane core and a barroisite/katophorite rim.

Fig. 7. Thin section images: a) D_1 fold in Monte Rosa micaschists preserving a pre-S_1 foliation; b) relict Hbl grains parly replaced by Chl +Qtz along the S_1 foliation. Back-scattered images of micaschist GR3: c) xenomorphic GrtI overgrown by GrtII which developed in the matrix too. The inset enhance a fracture (between arrows) in GrtI healed by GrtII. The A-A’ line shows the core-to-

rim profile of Fig. 8a; d) Qtz + Chl aggregate interpreted as pseudomorphs after Hbl; e) relict Hbl partly replaced by Qtz + Chl + Olig; f) particular of e).

Fig. 8. Minerals chemistry of sample GR3. a) chemical zoning core-to-rim profile of a garnet porphyroclast consisting of GrtI core overgrown by a GrtII rim; b) core-to-rim profile of a matrix GrtII showing a Grs-rich core similar in composition to the garnet filling the fractures of GrtI; c) chemical composition of garnet with arrow from core to rim of GrtII; d) chemical composition of white mica consisting of Pg, Ms and Phe with decreasing Si content from core to rim; e) chemical composition of the two chlorite generations; f) chemical composition of hornblende relict.

Fig. 9. a) PT pseudosection I for GR5 calculated with H_2O and SiO_2 saturated conditions for the composition reported in Table 3 (column A); b) contours for Alm, Grs and Prp showing that only the rim composition is stable; c) XMg in Gln; e) H_2O content in wt. %.

Fig. 10. a) PT pseudosection II for GR5 calculated with the same conditions of Fig. 9 and constraining the XMg of Gln to values ≥ 0.60; b) contours intersection for core and rim compositions of garnet. c) XJd and XMg contours for omphacite constraining the first exhumation step to 570-590 °C and 21-22 kbar. XJd increases quickly from 0.25 to 0.45 (0.30, 0.35 and 0.40 XJd curves are not represented for simplicity); d) Si content in phengite and XMg, $Al^{[IV]}$ and $Na^{[B]}$ in amphibole constraining the development of Barr to 13-15 kbar and max 610 °C; e) Grt rim isopleths intersection after fractionation of garnet core-mantle using the composition of column B of Table 3; f) Omp composition after fractionation of the Grt core-mantle.

Fig. 11. a) PT pseudosection for GrtI growth conditions of sample GR3 calculated for the composition of column C of Table 3; b) Grs, Pyr and Alm contours intersection for GrtI.

Fig. 12. a) PT pseudosection for GrtII and M3 assemblage growth conditions of sample GR3 using the composition in column D reported in Table 3; b) Grs, Pyr, Alm and Sps contours intersection for GrtII core; c) Grs, Pyr and Alm contours intersection for GrtII mantle and rim; d) Si content in phengite, XMg in Chl and XAn in plagioclase.

Fig. 13. a) PT pseudosection for GrtII and M3 assemblage growth conditions of sample GR3 using the feldspar solution model of Furman and Lindsley (1988) using the unfractionated composition of column D in Table 3; b) Grs, Pyr, Alm and Sps contours intersection for GrtII core c) Grs, Pyr and Alm contours intersection for GrtII mantle and rim; d) Si content in phengite, XMg in Chl and XAn in plagioclase.

Fig. 14. Alpine PT path reconstructed for the southern Monte Rosa Massif according to the results obtained from eclogite and metapelite samples. The PT paths of Borghi *et al.*, (1996) and Le Bayon *et al.* (2006) has been reported for comparison. The depth is calculated on the basis of an average density of 2.95 kgr/dm^3 for subducted crust.

Table 1. Selected microprobe analyses for eclogite GR5 from the southern border of the Monte Rosa Massif.

Table 2. Selected microprobe analyses for metapelite GR3 from the southern border of the Monte Rosa Massif.

Table 3. Chemical composition used to calculate the different pseudosection for the studied samples.

Figure 1

Click here to download high resolution image

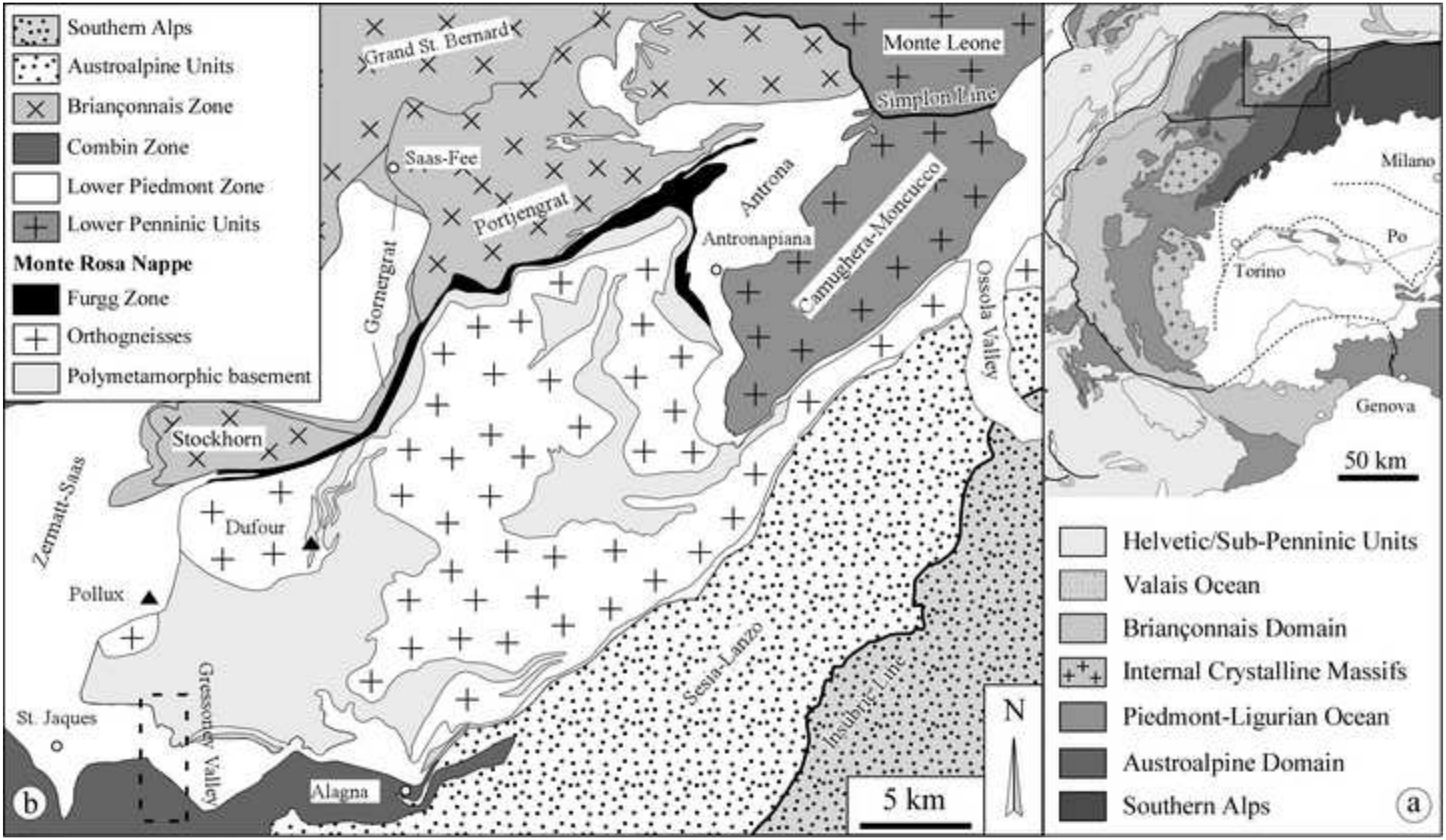

Figure 2

Click here to download high resolution image

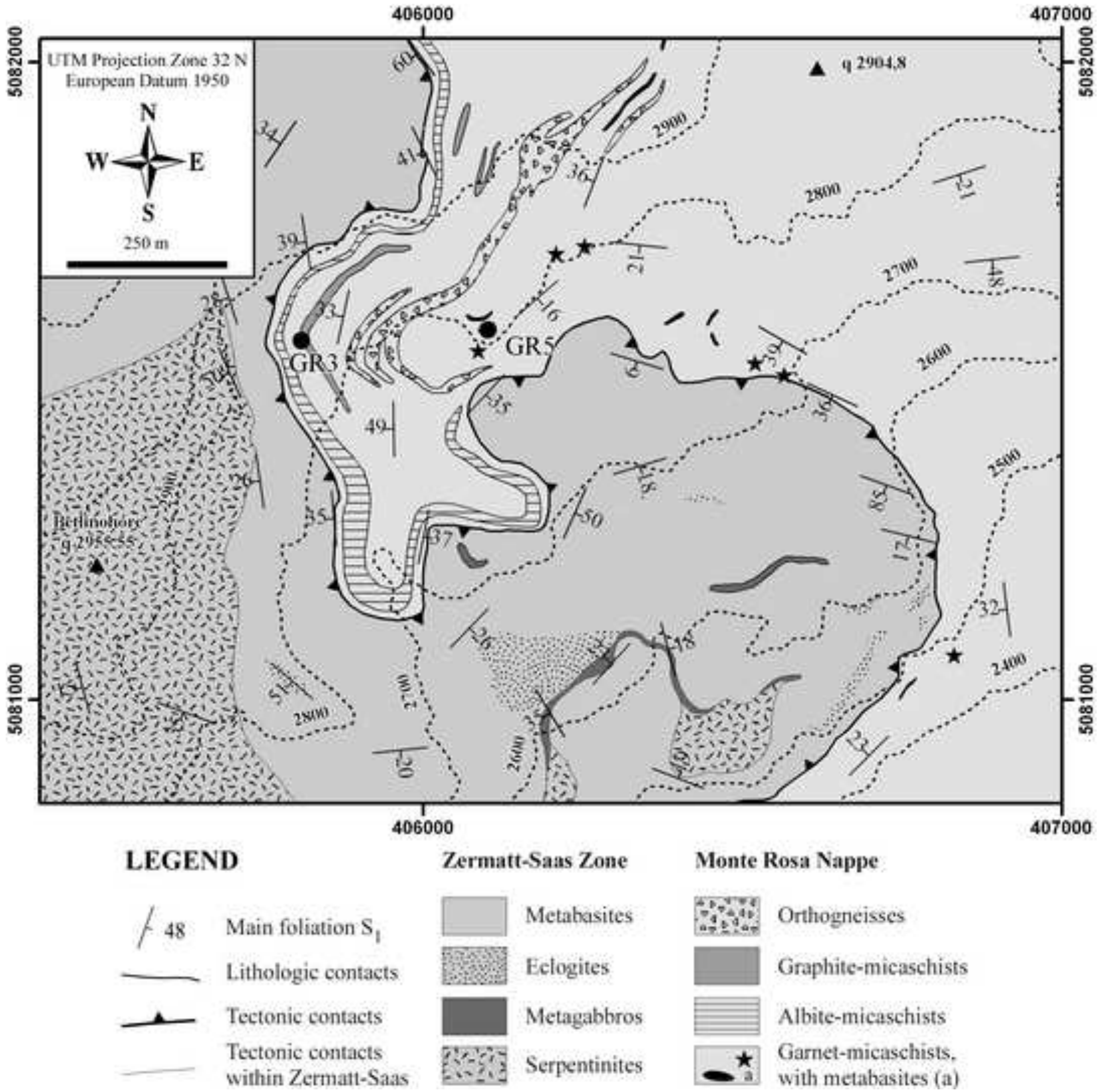

Figure 3

Click here to download high resolution image

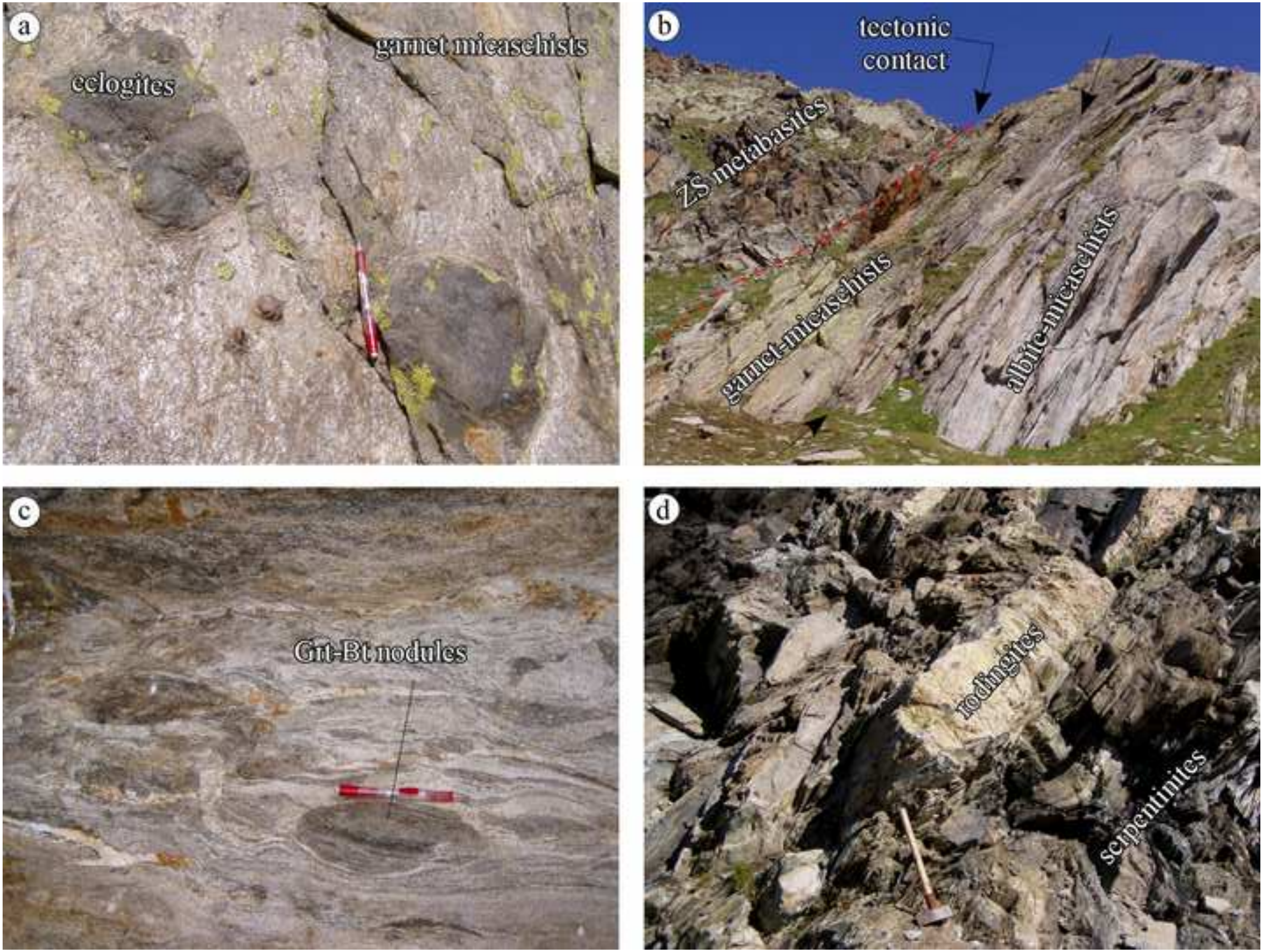

Figure 4

Click here to download high resolution image

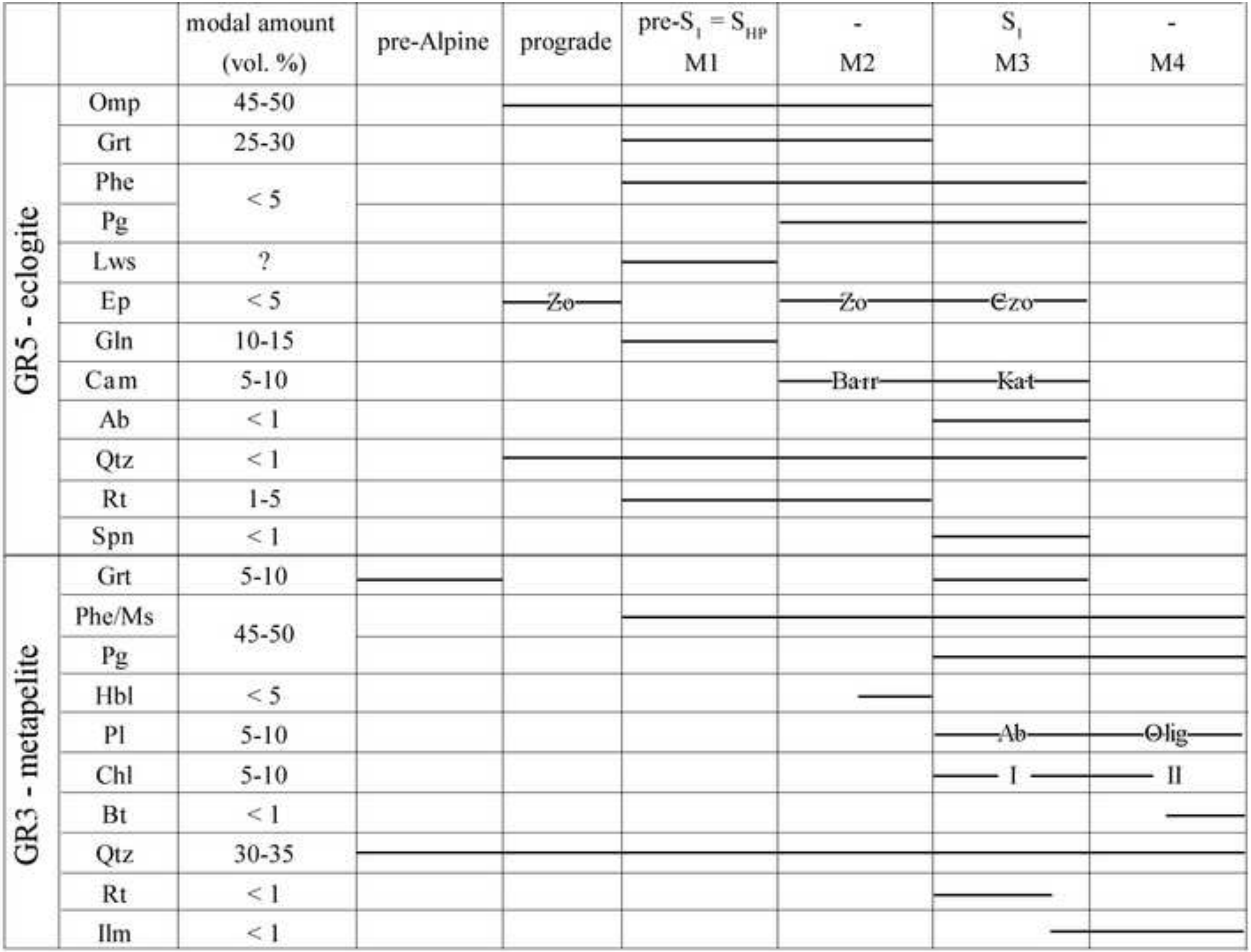

Figure 5
Click here to download high resolution image

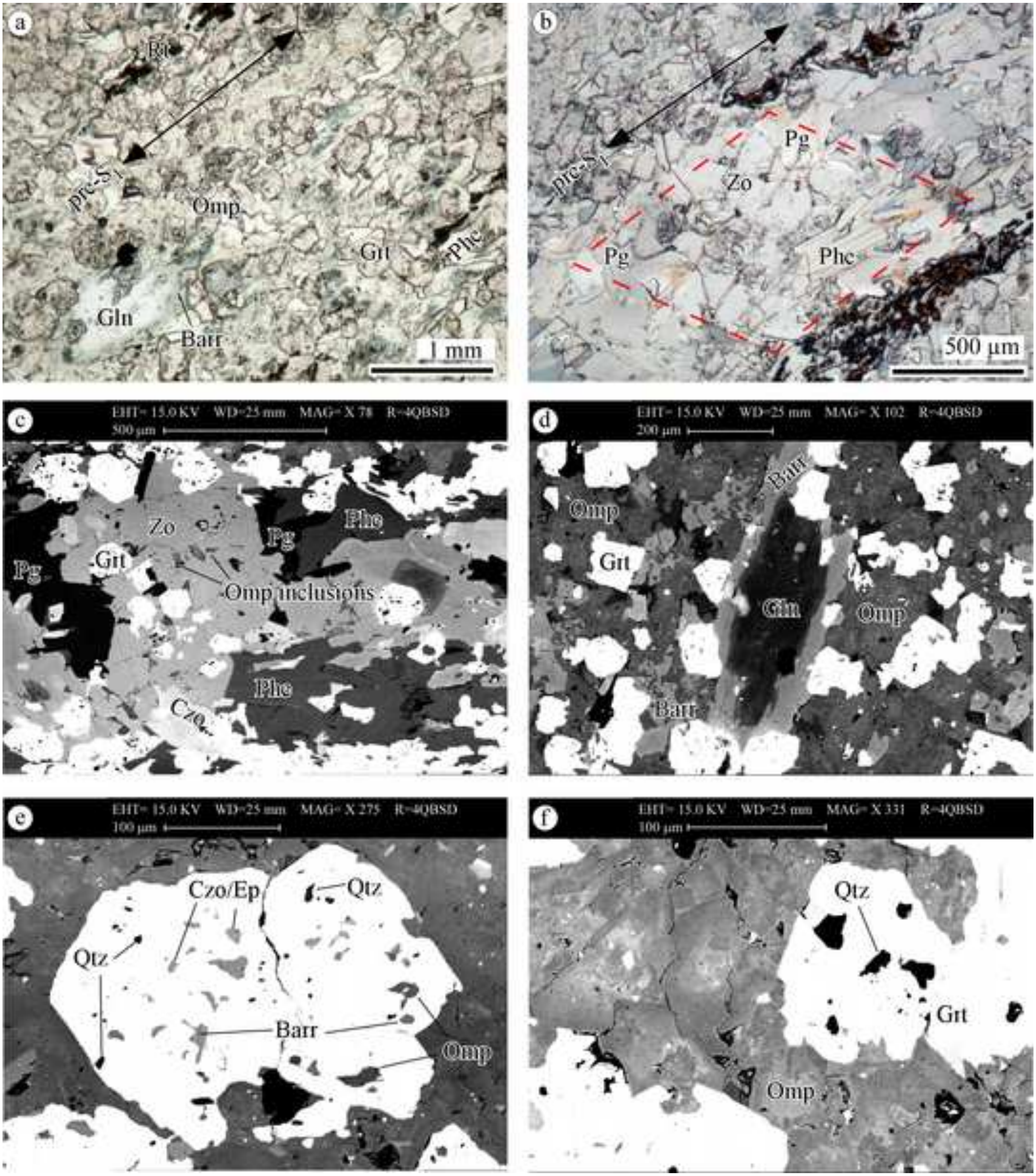

Figure 6

Click here to download high resolution image

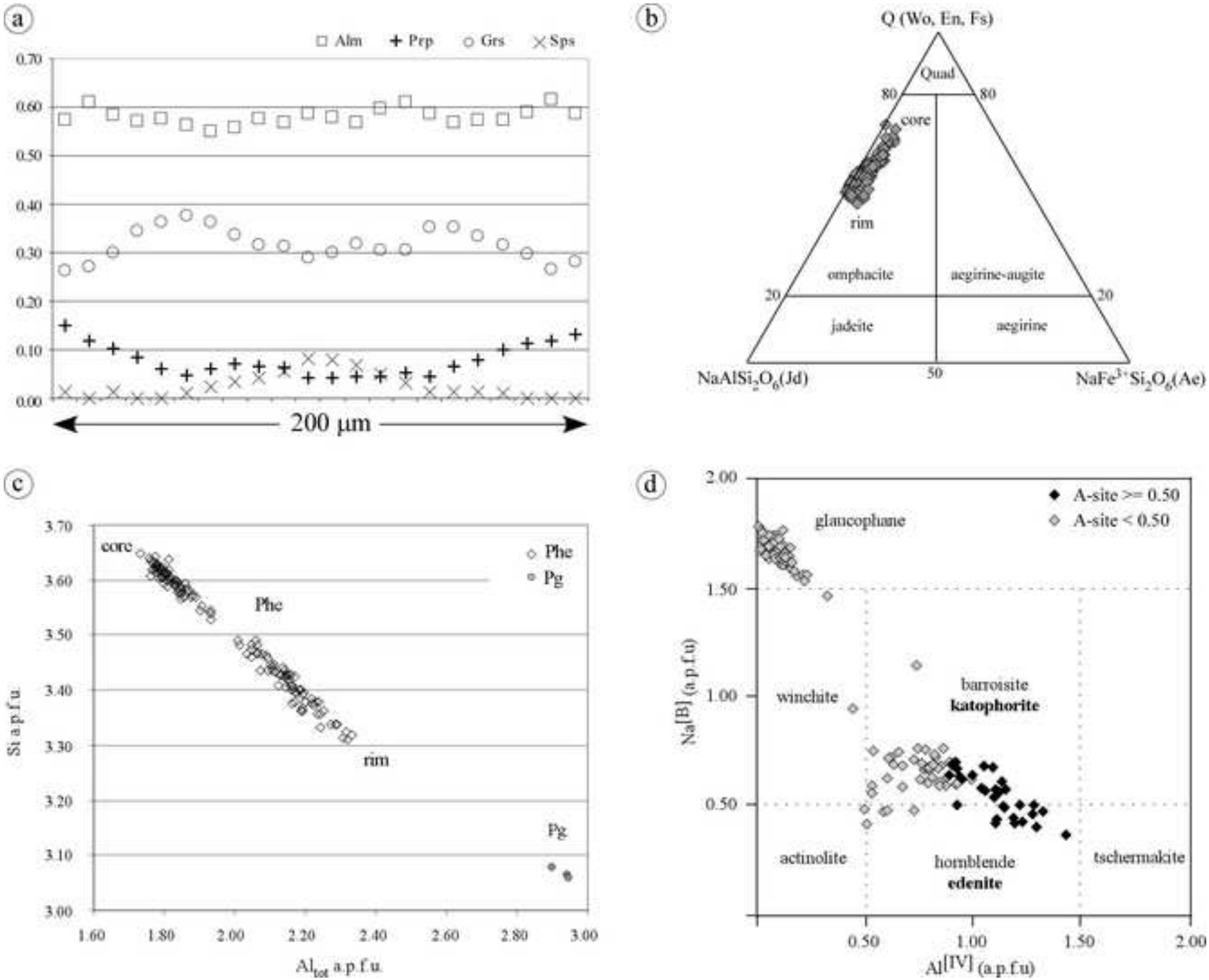

Figure 7
Click here to download high resolution image

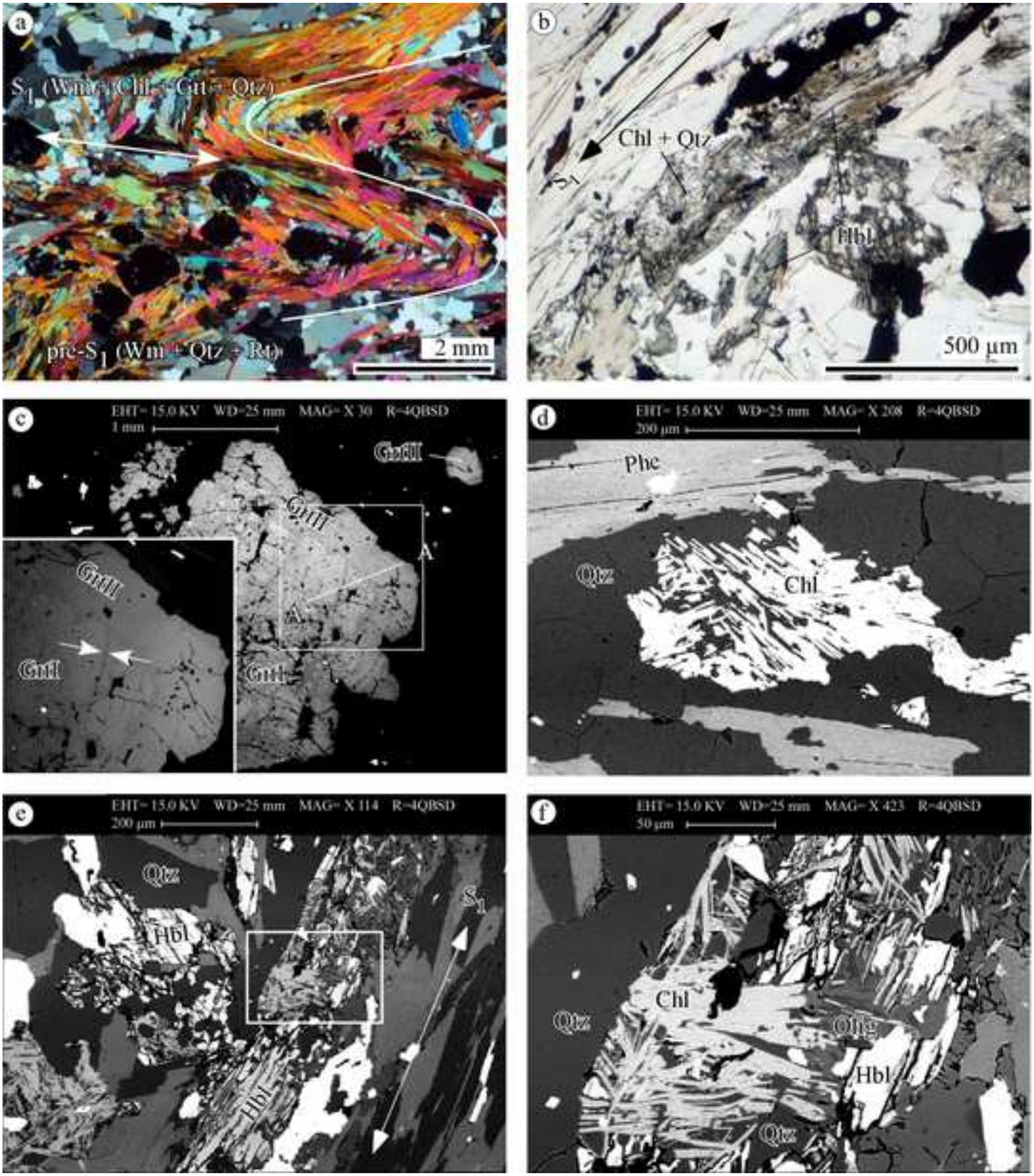

Figure 8

Click here to download high resolution image

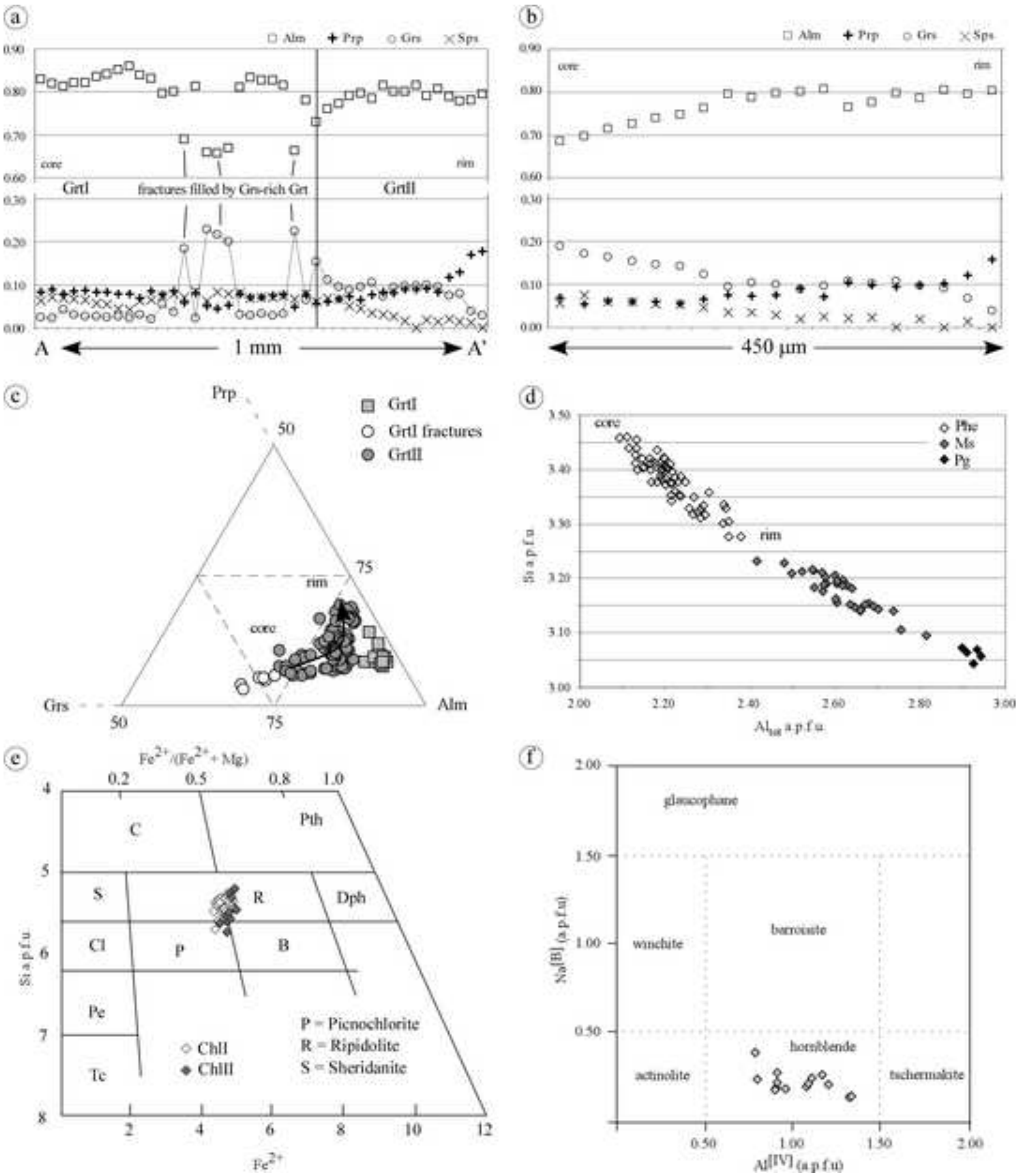

Figure 9

Click here to download high resolution image

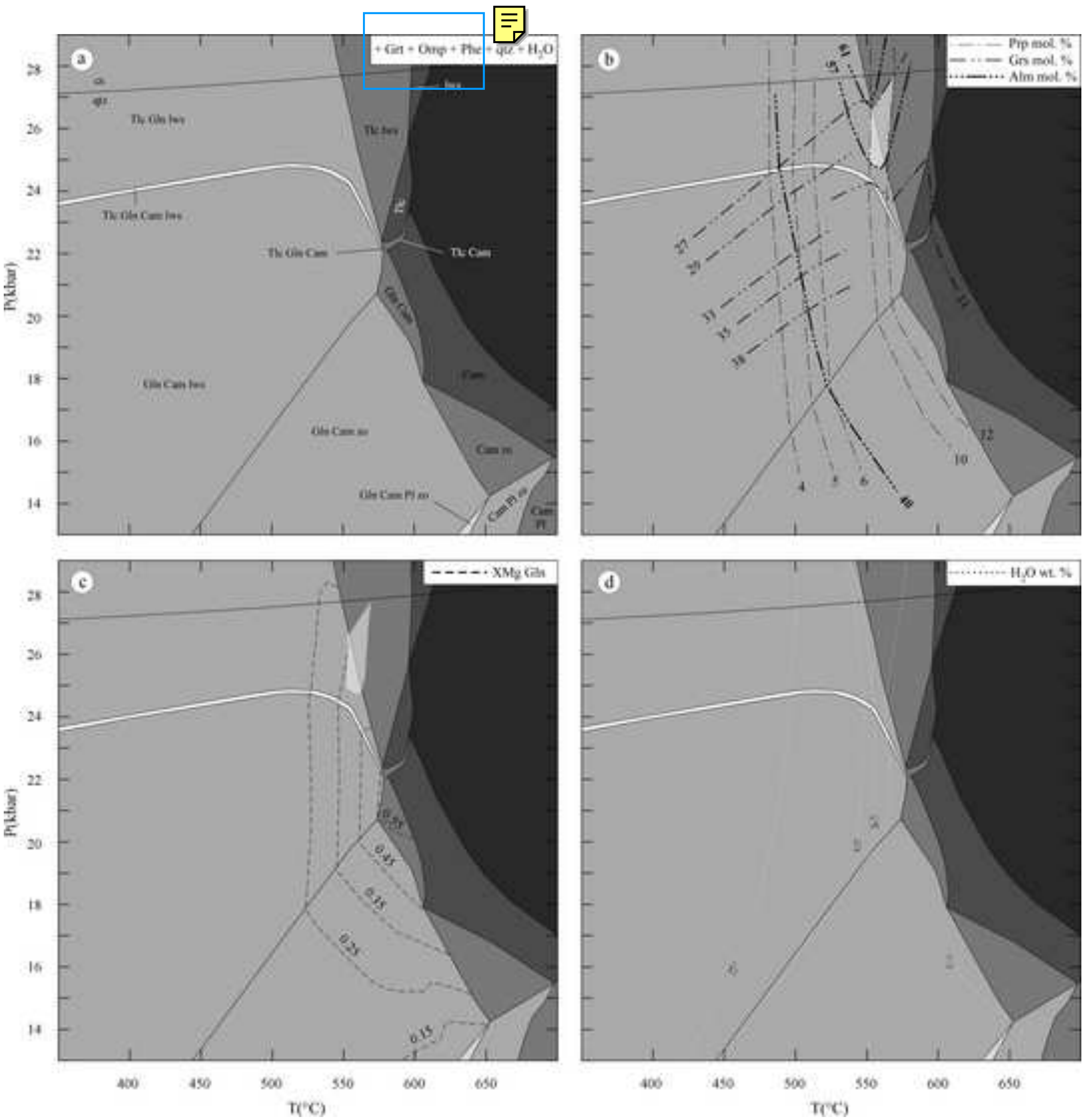

Figure 10

Click here to download high resolution image

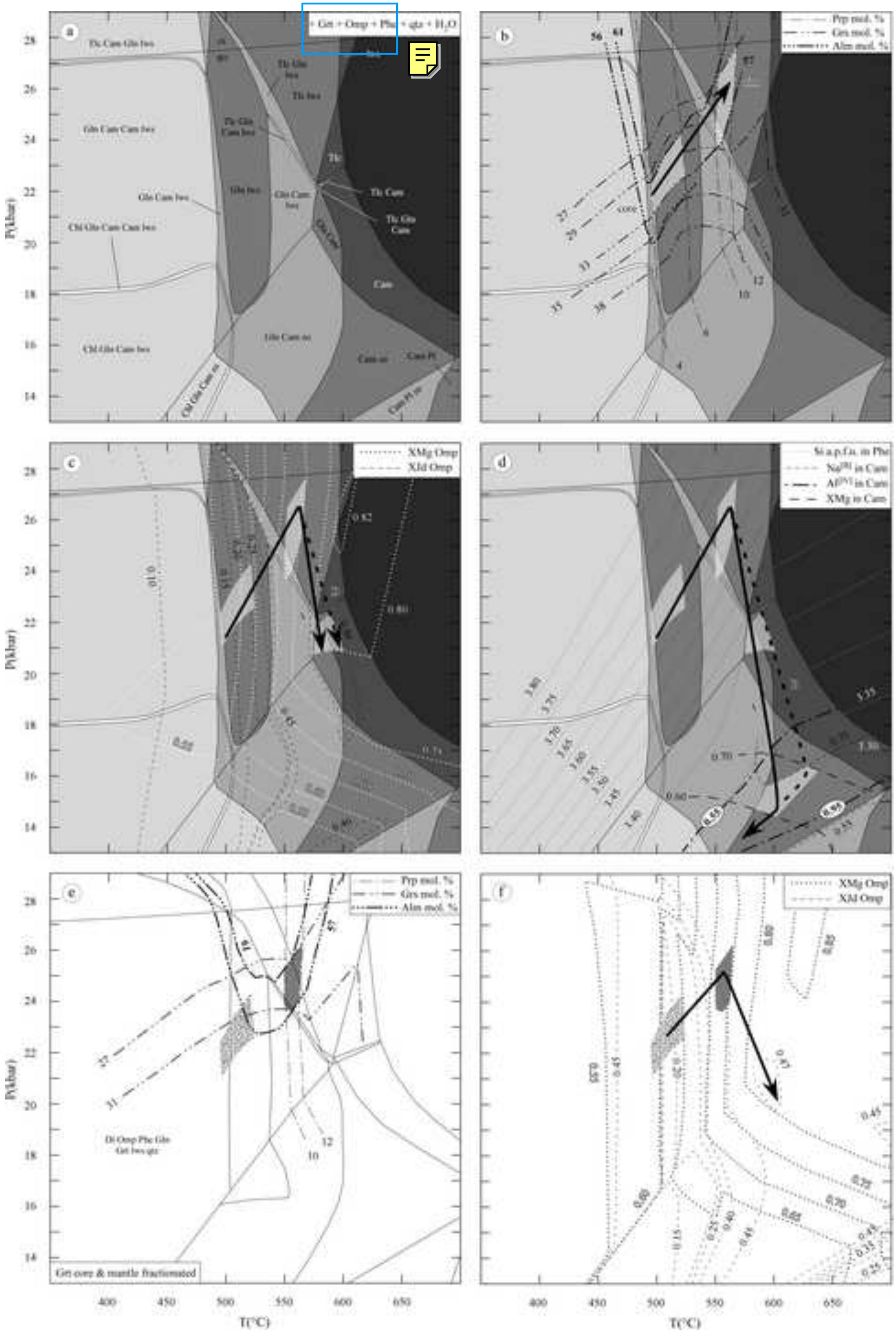

Figure 11

Click here to download high resolution image

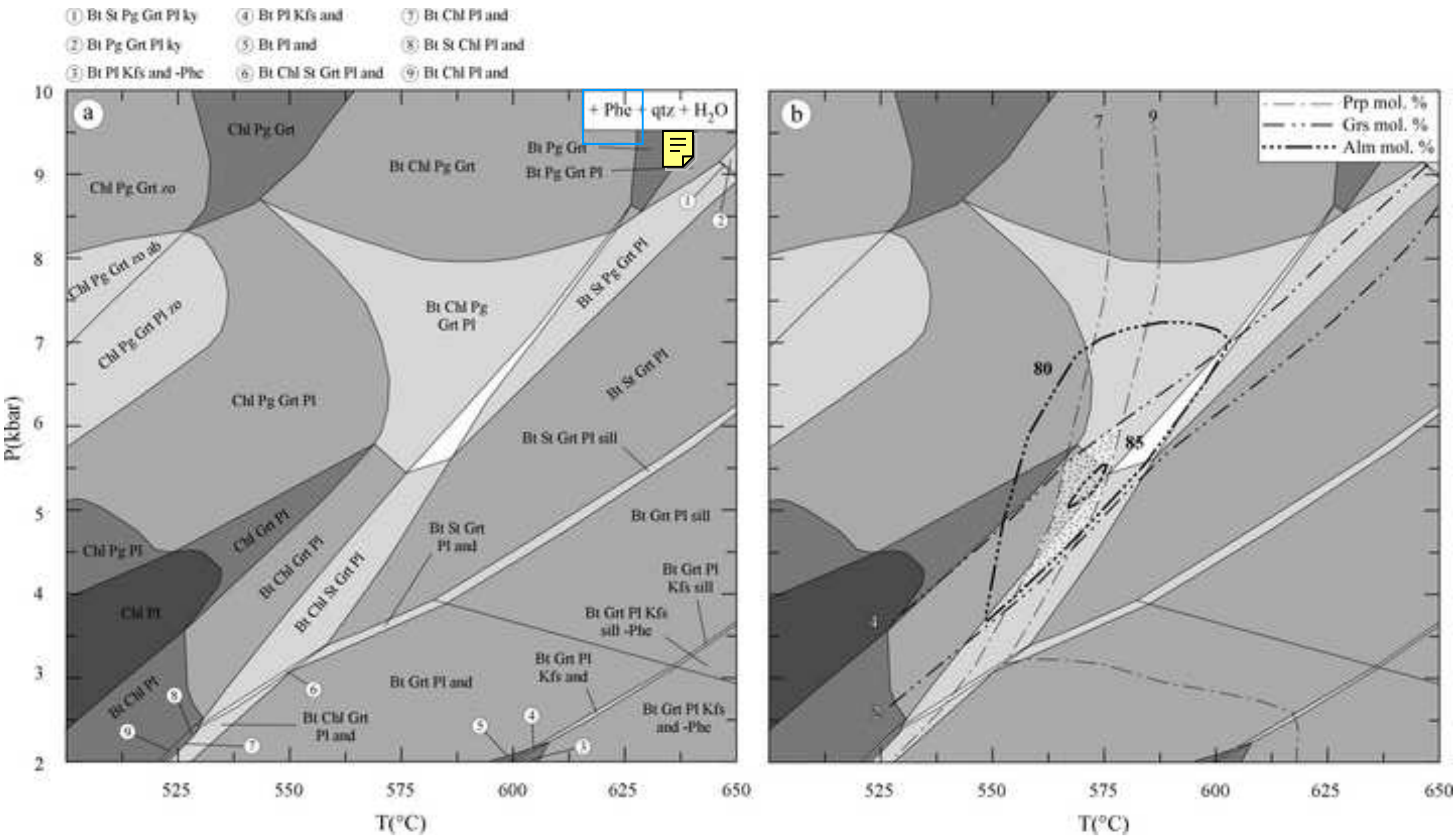

Figure 12
Click here to download high resolution image

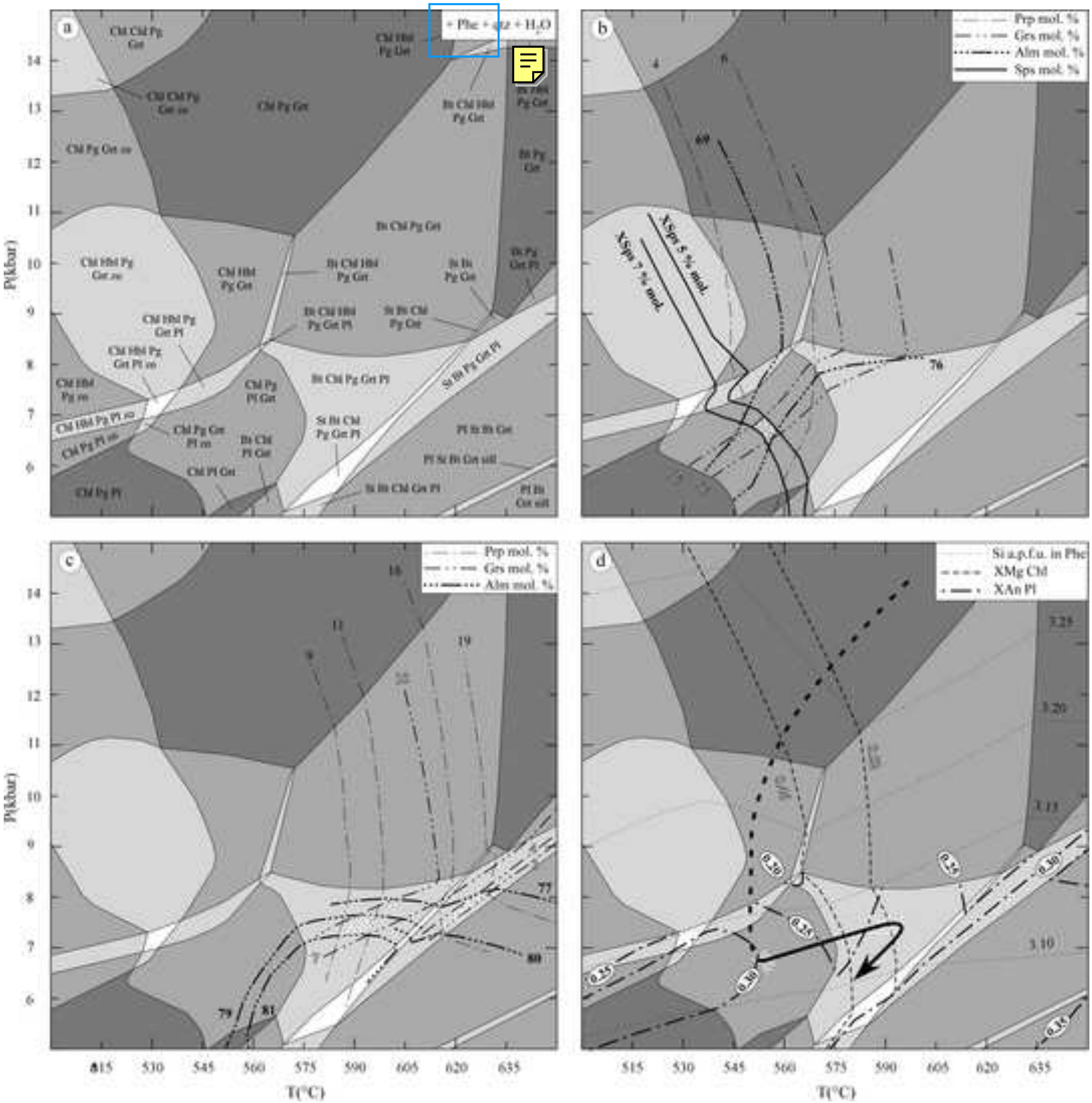

Figure 13

Click here to download high resolution image

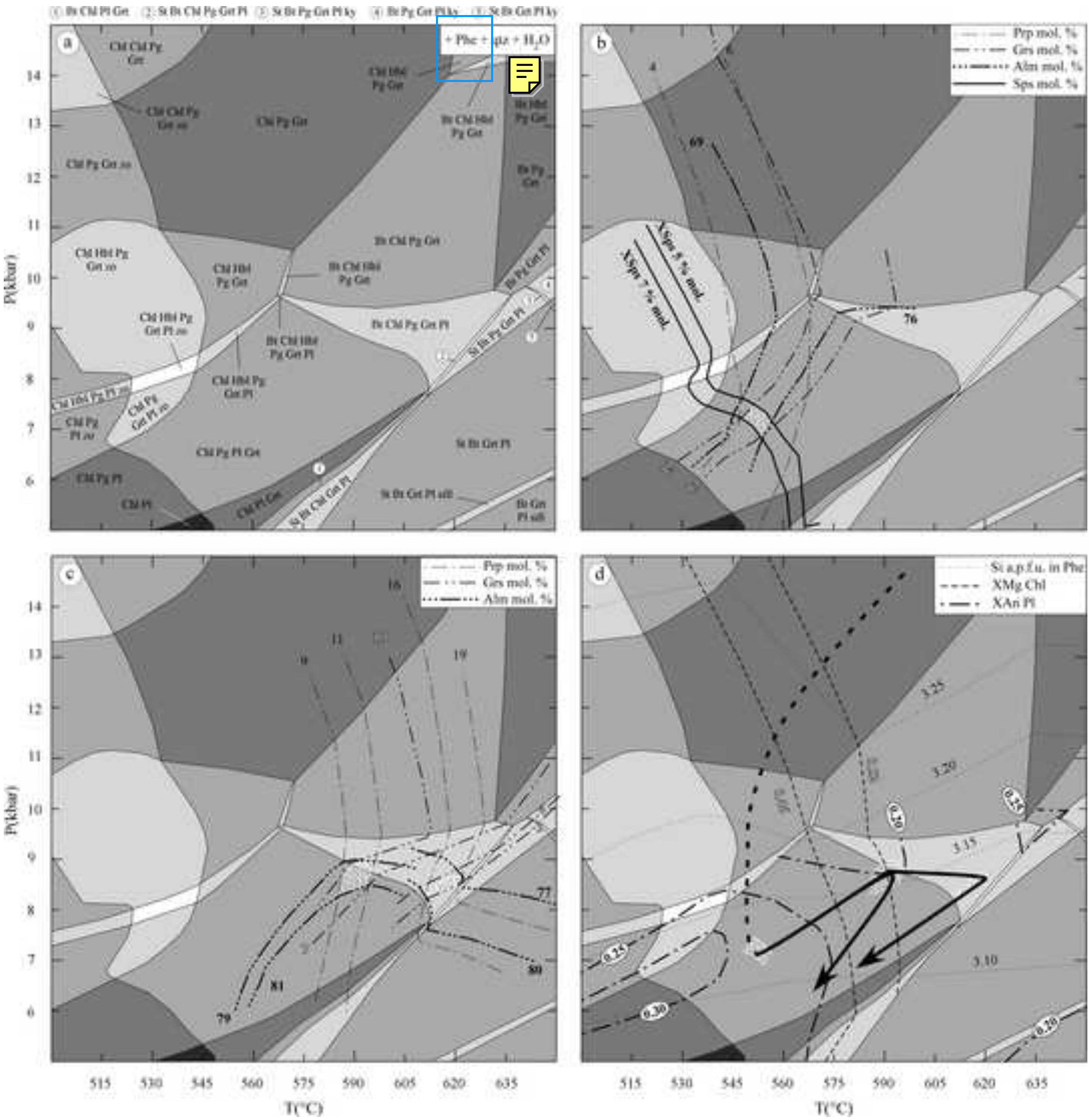

Figure 14
Click here to download high resolution image

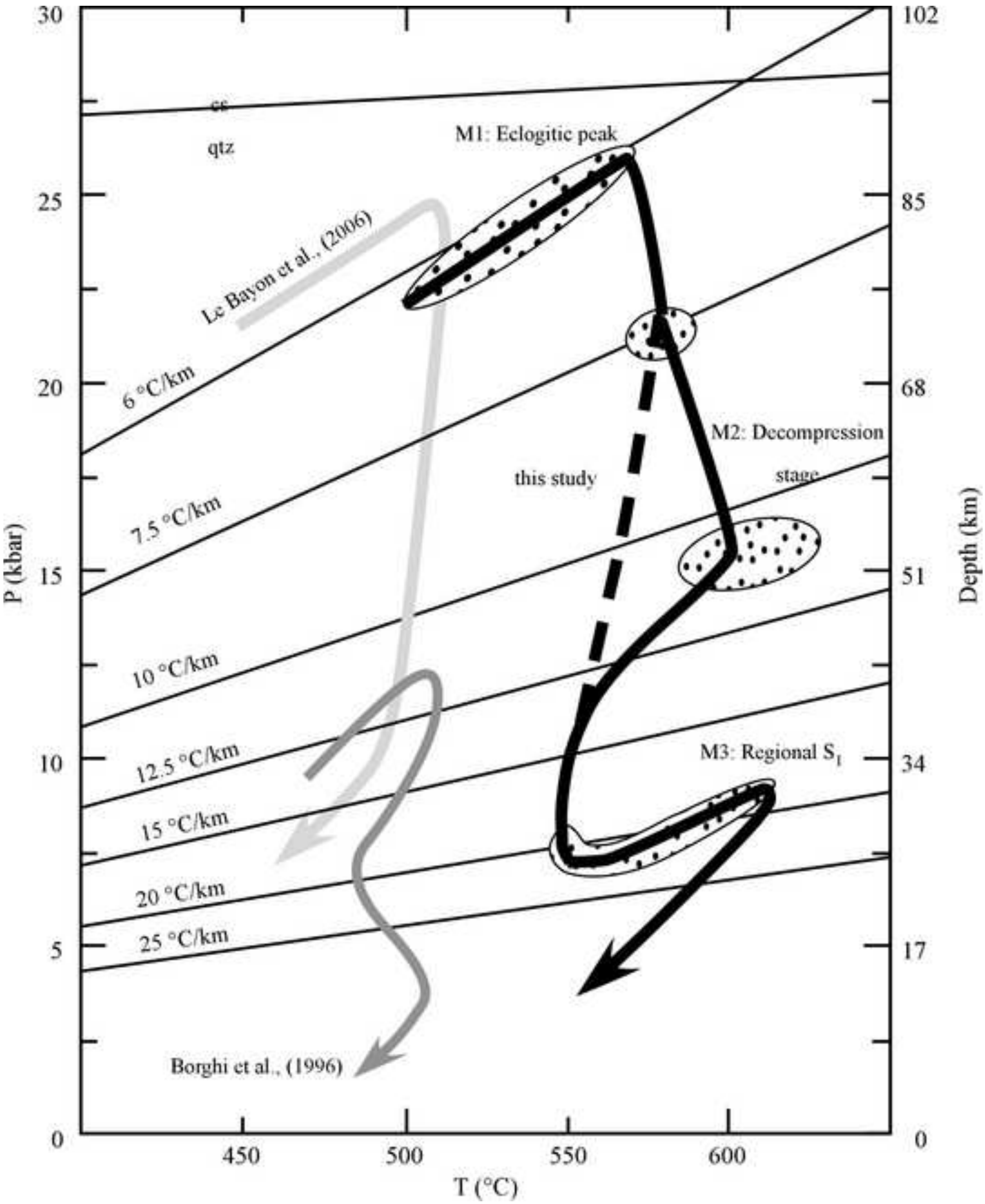

Table 1

Click here to download high resolution image

Analysis	Grt*		Omp**		Wm*			Am*		Zo***	Czo***
	gr200c	gr190r	omp1c	omp12r	wm14c	wm7r	wm116	am98c	am93r	zo27	ep20
Position	core	rim	core	rim	core	rim		core	rim		
					Phe	Phe	Pg	Gln	Barr		
SiO_2	37,40	37,43	55,71	56,35	54,89	51,08	48,61	59,24	49,64	39,69	39,14
TiO_2	0,00	0,00	0,00	0,00	0,00	0,00	0,00	0,00	0,00	0,00	0,00
Cr_2O_3	0,00	0,00	0,00	0,00	0,00	0,00	0,00	0,00	0,00	0,00	0,00
Al_2O_3	20,90	21,11	8,81	11,12	22,76	27,71	39,57	11,40	11,80	31,31	27,29
FeOtot	27,12	28,64	4,91	3,11	1,52	2,11	0,00	6,34	13,06	1,82	7,61
MnO	3,73	0,00	0,00	0,00	0,00	0,00	0,00	0,00	0,00	0,00	0,00
MgO	1,08	3,09	9,31	8,65	5,43	3,31	0,00	13,15	11,57	0,00	0,00
NiO	0,00	0,00	0,00	0,00	0,00	0,00	0,00	0,00	0,00	0,00	0,00
CaO	10,40	9,93	15,51	13,74	0,00	0,00	0,00	1,13	8,60	24,95	24,45
Na_2O	0,00	0,00	5,90	6,82	0,00	0,89	6,92	6,74	3,70	0,00	0,00
K_2O	0,00	0,00	0,00	0,00	11,52	10,50	0,84	0,00	0,32	0,00	0,00
Sum	100,63	100,20	100,15	99,79	96,12	95,60	95,94	98,00	98,69	97,77	98,49
Si	2,985	2,967	1,998	1,998	3,621	3,397	3,065	7,955	7,077	6,059	6,029
Ti	0,000	0,000	0,000	0,000	0,000	0,000	0,000	0,000	0,000	0,000	0,000
Cr	0,000	0,000	0,000	0,000	0,000	0,000	0,000	0,000	0,000	0,000	0,000
Al	1,966	1,972	0,372	0,465	1,770	2,172	2,942	1,804	1,984	5,635	4,956
Fe^{3+}	0,000	0,000	0,042	0,007	0,000	0,000	0,000	0,000	0,000	0,233	0,980
Fe^{2+}	1,811	1,899	0,105	0,085	0,084	0,118	0,000	0,712	1,558	0,000	0,000
Mn	0,252	0,000	0,000	0,000	0,000	0,000	0,000	0,000	0,000	0,000	0,000
Mg	0,129	0,365	0,498	0,457	0,533	0,328	0,000	2,631	2,459	0,000	0,000
Ni	0,000	0,000	0,000	0,000	0,000	0,000	0,000	0,000	0,000	0,000	0,000
Ca	0,890	0,844	0,596	0,522	0,000	0,000	0,000	0,163	1,313	4,081	4,037
Na	0,000	0,000	0,410	0,469	0,000	0,115	0,846	1,755	1,023	0,000	0,000
K	0,000	0,000	0,000	0,000	0,970	0,891	0,067	0,000	0,058	0,000	0,000
Sum	8,033	8,047	4,021	4,003	6,978	7,021	6,920	15,020	15,472	16,008	16,002

*assuming all ferrous iron; ** Fe3+ according to Lindsley & Anderson (1983); Fe3+ assuming Fe2O3 = FeO/0.9

Table 2

Click here to download high resolution image

	Grt*			Wm*				Chl*	Pl	Hbl*
Analysis	grt4c	grt64c	grt82r	wm34c	wm31r	wm50r	pg1	chl45c	pl43	am6
Position		core	rim	core	rim	rim				
	GrtI	GrtII	GrtII	Phe	Phe	Ms	Pg	Chl	Olig	Hbl
SiO_2	36,59	37,14	38,14	52,08	50,58	49,22	48,11	26,45	65,84	48,26
TiO_2	0,00	0,00	0,00	0,00	0,46	0,51	0,00	0,00	0,00	0,00
Cr_2O_3	0,00	0,00	0,00	0,00	0,00	0,00	0,00	0,00	0,00	0,00
Al_2O_3	19,95	19,98	20,46	28,41	28,58	34,63	38,48	21,64	21,34	10,68
FeOtot	36,93	36,80	36,10	1,53	2,33	1,10	0,73	26,66	0,00	16,37
MnO	3,08	3,22	0,62	0,00	0,00	0,00	0,00	0,00	0,00	0,00
MgO	2,00	2,82	3,11	2,99	2,87	1,01	0,00	14,54	0,00	11,52
NiO	0,00	0,00	0,00	0,00	0,00	0,00	0,00	0,00	0,00	0,00
CaO	1,47	0,63	2,42	0,00	0,00	0,00	0,00	0,00	2,72	8,46
Na_2O	0,00	0,00	0,00	0,61	0,64	0,95	6,93	0,00	9,57	1,11
K_2O	0,00	0,00	0,00	10,65	10,50	9,94	0,95	0,00	0,00	0,24
Sum	100,02	100,59	100,85	96,27	95,96	97,36	95,20	89,29	99,47	96,64
Si	2,997	3,011	3,043	3,420	3,353	3,182	3,073	5,480	2,900	7,090
Ti	0,000	0,000	0,000	0,000	0,023	0,025	0,000	0,000	0,000	0,000
Cr	0,000	0,000	0,000	0,000	0,000	0,000	0,000	0,000	0,000	0,000
Al	1,927	1,910	1,924	2,199	2,233	2,639	2,898	5,286	1,108	1,850
Fe^{3+}	0,000	0,000	0,000	0,000	0,000	0,000	0,000	0,000	0,000	0,000
Fe^{2+}	2,529	2,496	2,409	0,084	0,129	0,059	0,039	4,620	0,000	2,011
Mn	0,214	0,221	0,042	0,000	0,000	0,000	0,000	0,000	0,000	0,000
Mg	0,244	0,341	0,369	0,293	0,284	0,098	0,000	4,491	0,000	2,522
Ni	0,000	0,000	0,000	0,000	0,000	0,000	0,000	0,000	0,000	0,000
Ca	0,129	0,055	0,207	0,000	0,000	0,000	0,000	0,000	0,817	1,332
Na	0,000	0,000	0,000	0,077	0,082	0,119	0,858	0,000	0,128	0,315
K	0,000	0,000	0,000	0,892	0,888	0,820	0,078	0,000	0,000	0,046
Sum	8,040	8,034	7,994	6,965	6,992	6,942	6,946	19,877	4,953	15,166

*assuming all ferrous iron

Table 3
Click here to download high resolution image

	GR5		GR3	
	A	B	C	D
	XRF	*- Grt core* & mantle	*XRF*	*- GrtI core*
SiO_2	48.15	50.22	64.76	65.31
Al_2O_3	15.73	14.79	19.62	19.61
FeO	11.61	8.68	6.64	6.05
CaO	11.97	11.96	0.43	0.42
MgO	6.38	7.28	2.11	2.11
Na_2O	3.35	3.99	1.00	1.02
K_2O	0.49	0.58	4.14	4.22
MnO	0.29	0.08	0.10	0.04